

# **Impacts of trace components on Oxy-combustion for the Callide Oxy-fuel Project – Further results and analysis from Callide field trials, December, 2012**

Anthony L Morrison<sup>1</sup>, Peter F. Nelson<sup>1</sup>, P. Sargent Bray<sup>1</sup>,

<sup>1</sup>*Graduate School of the Environment, Macquarie University, Australia*

## ***FINAL REPORT***

***July 2014***



*The authors wish to acknowledge financial assistance provided through Australian National Low Emissions Coal Research and Development (ANLEC R&D). ANLEC R&D is supported by Australian Coal Association Low Emissions Technology Limited and the Australian Government through the Clean Energy Initiative*

## SUMMARY

It is recognised that the behaviour of trace metals and the related characteristics of the formation of fine particles may have important implications for process options, gas cleaning, environmental risk and resultant cost in oxy-fuel combustion. In spite of its potential importance to oxy-fuel combustion, the effects of firing in O<sub>2</sub>/CO<sub>2</sub> mixtures on trace metal deportment, speciation, and behaviour in flue gas cleaning systems have not been extensively studied. Environmental and operational risk will be determined by a range of inter-related factors including:

- The concentrations of trace metals in the gas produced from the overall process;
- Capture efficiencies of the trace species in the various air pollution control devices used in the process; including gas and particulate control devices, and specialised systems for the removal of specific species such as mercury;
- Gas quality required to avoid operational issues such as corrosion, and to enable sequestration in a variety of storage media without creating unacceptable environmental risks; the required quality for CO<sub>2</sub> transport will be defined by (future and awaited) regulation but may be at the standards currently required of food or beverage grade CO<sub>2</sub>; and
- Speciation of some trace elements

The last issue is particularly important as it is widely recognised that distribution, mobility and bioavailability of any element not only depends on the total concentration but, critically on the chemical forms and oxidation states of these elements. For example, the toxicity of Cr varies dramatically depending on whether it is present as Cr<sup>6+</sup> or Cr<sup>3+</sup>.

Macquarie University was engaged by the Australian National Low Emissions Coal Research and Development Ltd (ANLEC R&D) to undertake a research program to investigate the behaviour of trace elements during oxy-firing and CO<sub>2</sub> capture and processing. In December 2012, a test program was undertaken over a three week period on the retrofitted Callide A power plant with capability for both oxy and air-firing. During this period four coal feeds were combusted under both air-fired and oxy-fired conditions.

Gaseous and particulate sampling was undertaken in the process exhaust gas stream after fabric filtration at the stack and at various stages of the CO<sub>2</sub> compression and purification process. Solids samples collected from throughout the combustion and gas handling train were also extensively analysed.

The field trials were supported by laboratory work where combustion took place in a drop tube furnace and modelling of mercury partitioning using the iPOG model developed for United Nations Environment Program (UNEP) Coal Mercury Partnership. The measurements have provided detailed information on trace components of oxy-fired combustion gases and comparative measurements under air fired conditions, including:

- Trace metal and particulate matter (PM<sub>10</sub> and PM<sub>2.5</sub>) emission rates from oxy-combustion compared to air-fired systems – to allow environmental risk assessment of stack emissions from the Callide Oxy-Fuel Plant.

- Trace element speciation in air-fired and oxy-combustion products (gas, bottom and fly ash) for both mercury and chromium, to allow the toxicity, risk and environmental transport behaviour associated with these products to be assessed;
- Trace metal capture and transformation rates in the flue gas cleaning system and CO<sub>2</sub> processing plant;
- Ultimate trace component concentrations in product CO<sub>2</sub>,

In the project the target list of species to be characterised was based on the list of reportable substances included in the Australian National Pollutant Inventory (see <http://www.npi.gov.au/substances/list-of-subst.html>). Mercury was particularly targeted, given its importance from both a health and operational perspective.

### **Outcomes:**

Overall the project objectives were achieved and the results suggest that oxy-firing does not pose significantly higher environmental or operational risks than conventional air-firing. The levels of trace metals in the “purified” CO<sub>2</sub> gas stream should not pose operational issues within the CPU. The project was successful in meeting its scope and objectives.

A field campaign was held during the period 3<sup>rd</sup> – 20<sup>th</sup> December, 2012 with a focus on establishing the fate and possible operational impacts of trace elements in the Callide Oxyfuel processing plant. The field trials were followed by extensive chemical analysis of the product materials collected. The fieldwork was supported by laboratory combustion studies using a drop tube furnace to examine combustion under oxy-firing conditions using models of elemental enrichment previously used for air-fired systems.

Sampling was carried out during the field trials for solids inputs and outputs (coal and ash), gases at the stack exhaust (under both air and oxy-fired conditions) and at various points in the CO<sub>2</sub> Processing Unit (CPU). Four coal feeds were tested during the field trials under both air-fired and oxy-fired conditions, including a number of coal blends.

Levels of metals, SO<sub>x</sub> and mercury in particular, are below the level of operational concern in the CPU beyond the first low pressure scrubber. At the levels of these species measured the produced CO<sub>2</sub> would comply with the specifications for use in the food and beverage industry. However hydrocarbons, and a number of other species, including those of nitrogen, were not measured. Until these analyses have occurred it is not possible to unequivocally state that the product CO<sub>2</sub> would be acceptable for this use.

Modelling and measurement of mercury behaviour in the combustion system showed the strong relationship between carbon in flyash and mercury partitioning into the ash fraction. This may have implications which should be examined for plants which operate at higher efficiency and consequent lower carbon in ash. Approximately 80% of mercury in CPU process gas was removed by the initial low pressure scrubber; with the final CPU process gas mercury concentration approaching the concentrations measured in ambient air (<2 ng/m<sup>3</sup>).

An examination of total and environmentally available chromium (determined by an aggressive acid digestion) in all ash and coal samples from the field trials has shown levels are significantly lower than health based investigation levels for soils containing Cr of 100 mg/kg. It was also shown that 85-90% of the total chromium is isolated within the siliceous glass matrix of the ash and not available to leaching environmental fluids. The hexavalent

form of chromium [Cr(VI)] was below the normal limit of reporting of 0.5 mg/kg for all samples.

Halogens (Br, Cl and F) were at or below detection limits for the sampling techniques in both the stack and CPU. Halides (HBr, HCl and HF) were detectable in the stack (but not in the CPU), although no consistent trend in the field trial results between coal type or firing mode (oxy or air fired) was apparent. Research in the laboratory suggests that depletion of these species from the coal and ash occurs in all but the finest of particle sizes.

From the field trial results it does not appear that partitioning of trace metals to the gas phase at the stack is a function of either firing condition (oxy or air-firing) or coal type. Follow up laboratory studies have shown potential mechanisms via particle elemental enrichment for this behaviour, although a trend following oxy-firing to higher enrichment of trace elements in the ash for the smaller particles increasing with elemental increased volatility is also apparent.

Laboratory studies confirmed the almost complete depletion of sulfur from the ash samples, so the probable influence of feed coal sulfur on flue gas concentrations observed in the field trials is unsurprising.. Under air-firing conditions SO<sub>2</sub> concentrations in the field trials flue gases were three to four times lower than during oxy-firing, which is expected due to the concentrating effect brought about by the removal of nitrogen from the system. Concentrations of SO<sub>x</sub> in the CPU were less than the minimum detection limits (<MDLs), for both SO<sub>2</sub> and for SO<sub>3</sub> and demonstrate that the sulfur in the process gas stream has been removed effectively from the CPU process gas by the initial low pressure scrubber.

## TABLE OF CONTENTS

<b>SUMMARY.....</b>	<b>3</b>
Outcomes:.....	4
<b>LIST OF TABLES .....</b>	<b>7</b>
<b>LIST OF FIGURES .....</b>	<b>7</b>
<b>1. INTRODUCTION and CONTEXT .....</b>	<b>8</b>
1.1 Target Species .....	9
<b>2. WORK PROGRAM.....</b>	<b>9</b>
<b>3. FURTHER EXAMINATION OF SAMPLES FROM THE FIELD TRIAL.....</b>	<b>11</b>
3.1 Environmentally available chromium and chromium speciation.....	11
3.1.1 Presence of Cr in coal and ash .....	11
3.1.2 Chromium: ecological effects and effects on human health .....	11
3.1.3 Chromium determination and speciation .....	12
3.1.4 Chromium determinations in field trial ash and coal samples .....	13
3.1.5 Application of the chromium results to the Callide Oxy-fuel process .....	15
<b>4. ALLOWABLE LEVELS OF TRACE ELEMENTS IN CO<sub>2</sub>.....</b>	<b>18</b>
4.1 Food grade CO <sub>2</sub> .....	18
4.2 Pipeline Grade CO <sub>2</sub> .....	20
4.3 Implications of CO <sub>2</sub> quality for the Callide Oxy-fuel process .....	21
<b>5. PREDICTIVE METHODS FOR MERCURY CAPTURE DETERMINATION USING iPOG .....</b>	<b>22</b>
5.1 Inputs .....	22
5.2 Outputs .....	22
5.3 Uses of iPOG.....	24
5.4 iPOG Limitations .....	24
5.5 Application of iPOG to the Callide OxyFuel Plant data .....	25
5.6 Implications of the iPOG modelling for the Callide Oxy-fuel process.....	26
<b>6. SUPPORTING EXPERIMENTAL PROGRAMME .....</b>	<b>28</b>
6.1 Experimental Equipment.....	28
6.2 Gas atmospheres.....	29
6.3 Coal feed .....	29
6.4 Feed coal size and analyses .....	30
6.5 Analysis of MOUDI substrates retaining sized coal ash samples .....	32
6.6 Results and discussion of drop tube experiments.....	32
6.6.1 Enrichment Factor .....	33
6.6.2 GROUP I elements (Si, Ca, Ti, Fe, K) .....	34
6.6.3 GROUP II(a) elements (Co, Cu, Ni) .....	36
6.6.4 GROUP II(b) elements (Cr, Mn).....	38
6.6.5 GROUP II(c) elements (Pb, Zn).....	39
6.6.6 GROUP III elements (Br, Cl, S, Se) .....	40
6.7 Relevance of EF results to the Callide Oxy-fuel process .....	44
<b>7. CONCLUSIONS.....</b>	<b>45</b>
7.1 Project extension .....	45
7.2 Project Overall.....	46
<b>8. REFERENCES .....</b>	<b>48</b>
<b>Appendix A Photographs of collected substrates showing coal ash distribution .....</b>	<b>51</b>
<b>Appendix B IBA analysis of ash samples from drop tube experiments .....</b>	<b>54</b>

## LIST OF TABLES

Table 1 Results of ash and coal analyses for acid digestible chromium ( $\text{Cr}_{\text{AD}}$ ) (values are mg/kg) .....	16
Table 2 Results of ash and coal analyses for Cr(VI) (values are $\mu\text{g/kg}^2$ ) .....	17
Table 3: iPOG data inputs .....	23
Table 4: Characteristics of US and Australian bituminous coals.....	25
Table 5: Input data for iPOG calculations for the Callide OxyFuel Plant .....	27
Table 6 Coal analyses .....	31
Table 7 Categorisation of elements based on volatility behaviour .....	33
Table 8 Summary of changes in EF with coal ash particle size and combustion conditions...	42

## LIST OF FIGURES

Figure 1 Possible reaction mechanisms for the formation of leachable and non-leachable Cr(VI) and non-leachable Cr(III) during coal combustion .....	12
Figure 2 Comparison of total and acid digestible chromium in composited ash from Callide Oxy-fuel field trials, December 2012.....	15
Figure 3: An example of iPOG's output screen .....	24
Figure 4: Mercury retained in ash (%) as a function carbon in ash (LOI, %); measurements and predictions using iPOG for air and oxy-fired conditions .....	26
Figure 5 Drop tube furnace used in experimental program. ....	28
Figure 6 Schematic diagram of the drop tube furnace showing dimensions of furnace heating zones (Z1-Z3).....	29
Figure 7 Schematic diagram of fluidized feeder developed for the drop tube furnace. ....	30
Figure 8 EF of silicon in coal ash as a function of size $<10\ \mu\text{m}$ . ....	34
Figure 9 EF of calcium in coal ash as a function of size $<10\ \mu\text{m}$ . ....	34
Figure 10 EF of titanium in coal ash as a function of size $<10\ \mu\text{m}$ .....	35
Figure 11 EF of iron in coal ash as a function of size $<10\ \mu\text{m}$ .....	35
Figure 12 EF of potassium in coal ash as a function of size $<10\ \mu\text{m}$ .....	36
Figure 13 EF of cobalt in coal ash as a function of size $<10\ \mu\text{m}$ . ....	36
Figure 14 EF of copper in coal ash as a function of size $<10\ \mu\text{m}$ .....	37
Figure 15 EF of nickel in coal ash as a function of size $<10\ \mu\text{m}$ . ....	37
Figure 16 EF of chromium in coal ash as a function of size $<10\ \mu\text{m}$ .....	38
Figure 17 EF of manganese in coal ash as a function of size $<10\ \mu\text{m}$ .....	38
Figure 18 EF of lead in coal ash as a function of size $<10\ \mu\text{m}$ . ....	39
Figure 19 EF of zinc in coal ash as a function of size $<10\ \mu\text{m}$ . ....	39
Figure 20 EF of bromine in coal ash as a function of size $<10\ \mu\text{m}$ .....	40
Figure 21 EF of chlorine in coal ash as a function of size $<10\ \mu\text{m}$ .....	40
Figure 22 EF of sulfur in coal ash as a function of size $<10\ \mu\text{m}$ . ....	41
Figure 23 RF of selenium in coal ash as a function of size $<10\ \mu\text{m}$ . ....	41

# 1. INTRODUCTION and CONTEXT

Carbon dioxide capture and sequestration and storage (CCS) has been proposed as a mechanism to reduce carbon dioxide emissions from the industrial use of fossil fuels to produce electricity and other services. Oxy-combustion is a candidate technology for CCS, and a demonstration of this technology is being undertaken through the Callide Oxy-fuel Project. (<http://www.callideoxyfuel.com/What/CallideOxyfuelProject.aspx>).

A potential component of the overall risk associated with oxy-combustion will be due to residual trace species in the CO<sub>2</sub> stream as these trace species will determine the need for and costs associated with gas-cleaning protocols for oxy-combustion to avoid emissions issues, and corrosion problems. It is recognised that the behaviour of trace metals and the related characteristics of the formation of fine particles may have important implications for process options and resultant cost (Toftegaard *et al.* 2010).

Environmental and operational risk of trace elements in oxyfuel processing will be determined by a range of inter-related considerations including:

- The emission flux (mass/time) of trace metals from the overall process;
- Capture efficiencies of the trace species in the various air pollution control devices used in the process; these may include gas and particulate control devices, and specialised systems for the removal of specific species such as mercury;
- Gas quality required to avoid operational issues such as corrosion, and to enable sequestration in a variety of storage media without creating unacceptable environmental risk; and
- Speciation of trace species

A detailed review of the possible impacts of trace elements from coal combustion on the oxyfuel process has been prepared for ANLEC R&D as an initial part of this project (Nelson 2013). Wall *et al* (2013) also identified gas quality as an early research and regulatory issue, as the gas produced from oxy-fuel has higher levels of inert gases, sulfur and nitrogen gases, and other trace impurities. A detailed knowledge of the impacts of gas quality on power plants and materials, on transport systems, and on the regulations imposed on gas quality for storage, is thus required to reduce the risk of this CCS technology, as the cost of gas cleaning is likely to be higher for oxy-fuel than for other carbon capture technologies (Wall *et al.* 2013).

Based on the earlier work outlined above it is clear that a significant component of the risk associated with oxy-combustion may be due to trace species in the CO<sub>2</sub> stream. These trace species will have an impact on costs associated with gas-cleaning requirements for oxy-combustion to avoid emissions and operational issues, such as corrosion. In the current project a combination of field measurements complemented by laboratory experiments, modelling and computational studies were carried out to obtain detailed information on trace components of oxy-fired combustion gases, including:

- Trace metal, gas and fine particulate matter (PM) emission rates from oxy-combustion compared to air-fired systems, to provide information for environmental risk assessment of stack emissions from the Callide Oxy-Fuel Plant; noting that, in fully



commercial plants there are not expected to be any stack emissions (although plants would be expected to be able to operate and be compliant in both firing modes);

- Trace metal speciation in oxy-combustion products (flue gas, bottom ash and fly ash); speciation determines the toxicity, environmental transport behaviour and hence the risk associated with these products;
- Trace metal capture and transformation rates in the flue gas cleaning system and CO<sub>2</sub> processing plant;
- Ultimate trace component concentrations in product CO<sub>2</sub>, and an assessment of the suitability of the CO<sub>2</sub> for various uses (eg, pipeline quality for transport and storage; comparison with food grade CO<sub>2</sub> and required additional cleaning required to meet food grade standards); and
- Physical modelling and computational studies to assess flue gas composition effects on CO<sub>2</sub> capture, and to support, through predictive capability, the next stage of commercialisation.

### **1.1 Target Species**

There are a number of accepted listings of trace metals and elements of environmental and/or human health concern. These include priority lists developed by the USEPA and by the Commonwealth for its Air Toxics Program. In the present work the target list of species to be characterised was based on the list of reportable substances included in the Australian National Pollutant Inventory (see <http://www.npi.gov.au/substances/list-of-subst.html>). The target element list for the project was:

- Antimony (Sb)
- Arsenic (As)
- Beryllium (Be)
- Boron (B)
- Cadmium (Cd)
- Chromium (Cr)
- Cobalt (Co)
- Copper (Cu)
- Lead (Pb)
- Manganese (Mn)
- Mercury (Hg)
- Nickel (Ni)
- Selenium (Se)
- Zinc (Zn)

## **2. WORK PROGRAM**

A series of measurements of trace element concentrations at the 30 MW Callide A Oxy-fuel plant were undertaken in the period 3<sup>rd</sup> – 20<sup>th</sup> December, 2012. Although the program had originally been planned to take place as two field campaigns in May, 2012 and April, 2013 these were compressed into one extended campaign by agreement with Callide Oxyfuel Services Pty Ltd (COSPL) and ANLEC R&D.

The field campaign involved personnel from Macquarie and Newcastle Universities, Malfroy Environmental Strategies and a contracted four person, specialist stack testing team (ECS Pty Ltd).

That component of the overall ANLEC R&D project 6-0411-0130 examined trace element transformations in the flue gas of the retrofitted Callide A power plant and CO<sub>2</sub> Processing Unit (CPU) during oxy and air-firing, to examine reactions between gas and particulate phases, and to determine trace element capture efficiencies in air pollution control devices. Details of the plant can be found on the Callide Oxyfuel website:  
<http://www.callideoxyfuel.com/What/CallideOxyfuelProject.aspx>

During the three week period of the field trial program, four coal feeds, including coal types from three coal deposits were combusted under both air-fired and oxy-fired conditions. The feed coals are characterised as a sub-bituminous coal (CL), a medium volatile bituminous coal (MN) and a semi-anthracitic coal (BL), Blend 1 (was a mixture of CL and BL coals), Blend 2 (a mixture of CL and MN coals), along with feeds of unblended CL and MN coals. Sampling was carried out for solids inputs and outputs (coal and ash), gases at the stack exhaust (under both air and oxy-fired conditions) and at various points within the CPU. The results from the field studies were reported in detail in the previous report (Morrison et al. 2014).

This report extends some of the work already reported to include:

- A detailed assessment of the environmental availability of chromium and the speciated hexavalent chromium form in the ash samples generated during the field trials.
- A comparison of the analysis of trace elements in CO<sub>2</sub> produced during the field trials benchmarked against pipeline and food grade CO<sub>2</sub> standards.
- Quantitative modelling of mercury emissions using the iPOG software package developed in conjunction with the United Nations Environment Program (UNEP) Mercury Partnerships. Input data for the model were the plant conditions measured during the field trial.
- Experimental work on elemental enrichment factors (EFs) in the finer particle sizes (<10 µm) produced during combustion and their implications for oxy-firing..

### **3. FURTHER EXAMINATION OF SAMPLES FROM THE FIELD TRIAL**

#### **3.1 *Environmentally available chromium and chromium speciation***

Along with metallic chromium ( $\text{Cr}^0$ ), chromium can exist in a range of oxidation states from  $\text{Cr}^{2+}$  to  $\text{Cr}^{6+}$ , but the commonly found forms in nature are trivalent, Cr(III) and hexavalent, Cr(VI) (Nriagu and Nieboer 1988).

##### **3.1.1 Presence of Cr in coal and ash**

In coals, chromium is usually found at low levels and ranges from <0.5- 100 mg/kg worldwide, although particular seams and areas can be orders of magnitude higher, these occurrences often being associated with the occurrence of chromite minerals ( $\text{FeCr}_2\text{O}_4$ ) (Finkelman 1999; Goodarzi and Huggins 2005). Levels in NSW and Queensland coals are typically somewhat lower than the worldwide averages of less than 1.5 - 30 mg/kg, while Victorian lignites are lower still at 0.08 - 19 mg/kg and Western Australian sub-bituminous coals have a significantly wider range 5 - 119 mg/kg (Swaine and Goodarzi 1995).

Work by several groups suggests that in both sub-bituminous and bituminous coals, chromium is present predominantly as Cr(III); illite (a clay mineral) features with some of the chromium in sub-bituminous coals derived from poorly crystallized chromium oxyhydroxide contained with organic macerals. In bituminous coals this latter source appears not to be present or detectable (Goodarzi and Huggins 2005; Stam et al. 2011).

The work by Stam et al. (2011) proposes that most (or all) of the Cr-illite minerals melt forming aluminosilicate glass phases in the flyash which are highly resistant to leaching. Whereas physical absorption on particle surfaces is suggested as the major mechanism for capture of Cr(VI) by flyash, following partial volatilisation during combustion, when organically bonded chromium is present in coal during combustion (Stam et al. 2011; Zhao et al. 2013). Figure 1 shows schematically a proposal for the formation of both leachable and non-leachable Cr(VI) and non-leachable Cr(III) from both the Cr-illite forms and organically bound Cr.

Deposition levels of Cr (VI) in fly ashes are typically very low, <3-6% of the total chromium and is often undetectable at these levels (Stam et al. 2011).

##### **3.1.2 Chromium: ecological effects and effects on human health**

Hexavalent chromium [Cr(VI)] is rare in nature and a non-essential metal for microorganisms and plants towards which it is highly toxic, causing effects to plant growth and development and alterations to the germination process (Shanker et al. 2005; Darakas et al. 2013; Dhal et al. 2013). In plants, the uptake and resultant toxicity is dependent on the presence of the speciated form [Cr(VI)] which controls its level of mobilisation (Shanker et al. 2005). Conversely, chromium (in the Cr(III) form) is an essential nutrient for mammalian function, and chromium deficiencies have long been implicated in the presence of diabetic and related conditions (Rabinowitz et al. 1983; Davis and Vincent 1997; Vincent 2004). The Cr(VI) form

is classified by the USEPA as a Group A human carcinogen as it is believed to be a cause of conditions ranging from lung cancer to kidney and gastric damage (Kimbrough et al. 1999). Although the most significant sources of chromium in the environment are deliberate use of chromium containing compounds in industries such as tanning, plating and steel manufacture, coal combustion by-products such as fly ash can be a significant source of the chromium introduced into the environment if ash repositories are poorly managed ((Nriagu and Nieboer 1988; Kimbrough et al. 1999; Kingston et al. 2005). As pointed to earlier, chromium is a common coal constituent, and the presence of some level of chromium (in all valence states) in power station flyash appears inevitable, although much is captured by particulate removal devices (Goodarzi and Huggins 2005; Zhao et al. 2013). The leaching of this chromium from ash repositories is highly dependent on climatic conditions (wet *versus* arid) (Kingston et al. 2005). Darakas *et al.* (2013) have confirmed earlier results that the release of Cr(VI) from flyash is controlled by pH and is more likely to occur under basic conditions.

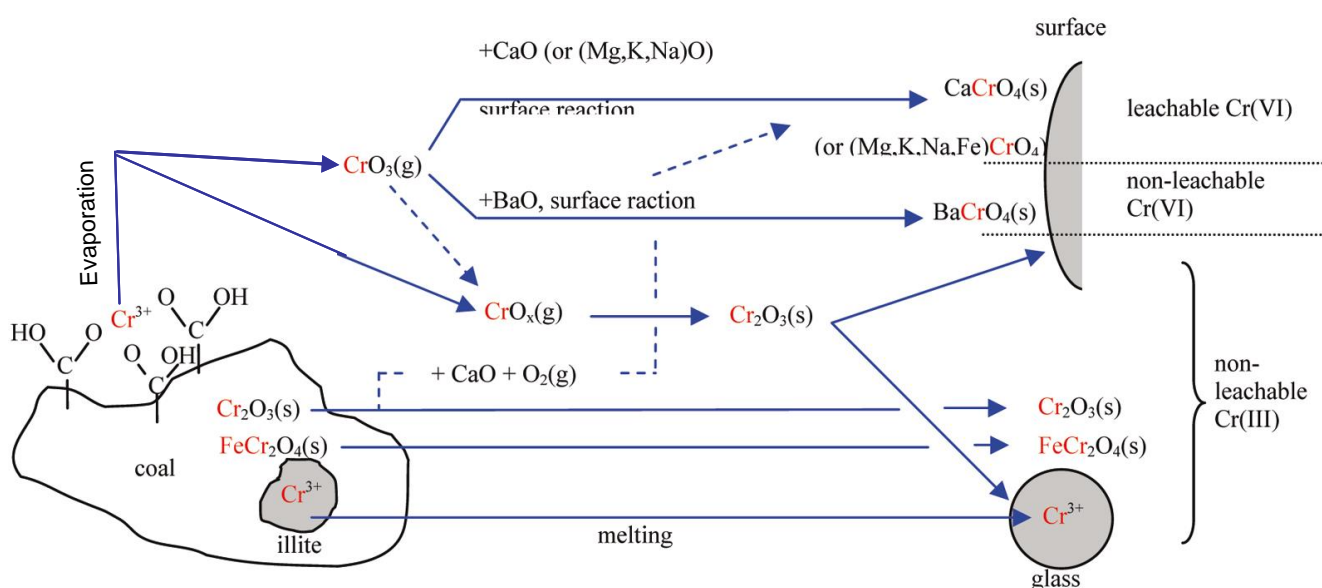


**Figure 1 Possible reaction mechanisms for the formation of leachable and non-leachable Cr(VI) and non-leachable Cr(III) during coal combustion [adapted from Stam *et al.* (2011) ]**

### 3.1.3 Chromium determination and speciation

While total chromium can be detected down to low levels ( $<0.1$  mg/kg), the quantification of the hexavalent chromium species (Cr(VI)) is made more challenging as it involves an extraction step which must dissolve the Cr(VI) species completely and avoid reduction of Cr(VI) to Cr(III) whilst this is achieved. USEPA Method 3060A uses a technique for Cr(VI) determination where the samples are exposed to a combination of  $\text{Na}_2\text{CO}_3$  and  $\text{NaOH}$  with continuous swirling and heating at  $95^\circ\text{C}$ . This solution has a pH of  $>12$  which should maintain stability of the Cr(VI) (USEPA 1996a). Although it has been established that the matrices of some materials result in artificially low Cr(VI) levels being determined using this method (Malherbe et al. 2011). This should not be the case with fly ashes as the problem seems to occur as a result of entrapment of Cr(VI) species and the formation and deposition mechanisms proposed for Cr(VI) in combustion systems (described previously) would seem to preclude this possibility.

Sophisticated techniques, such as x-ray detection near edge structure spectroscopy (XANES), requiring the use of a synchrotron, have been used for detection of Cr(VI) and determination of the ratio of Cr(VI)/Cr(III) in various materials, including coals and furnace ash (Huggins et al. 2000; Goodarzi and Huggins 2005; Stam et al. 2011). However given that the limit of detection of Cr(VI) for the technique appears to be ~10 mg/kg (Shaffer et al. 2001), its use for the quantification of furnace ash (fly ash and bottom ash) from power station coal combustion would appear restricted. This occurs because the Cr(VI) levels even in higher chromium coals [say an estimate of 6% of 100 mg/kg, or 6 mg/kg Cr(VI) (Stam et al. 2011)] are likely to be below the XANES detection limit. Because XANES is a solid state detection method what it does allow, at least in samples (not necessarily coals or ashes) containing a higher level of Cr(VI), is confirmation (or otherwise) of the effectiveness of the extraction method used in EPA3060A (Malherbe et al. 2011).

### **3.1.4 Chromium determinations in field trial ash and coal samples**

Total acid digestible chromium ( $\text{Cr}_{\text{AD}}$ ) and hexavalent forms of chromium (Cr(VI)) were determined on all coal and all ash samples collected during the December 2012 oxyfuel field trials at Callide. These included all fly ash hoppers, furnace (bottom) ash and ash samples from the rear pass and air heater collection points, 193 samples in total were analysed. The analyses were carried out by the Australian Government National Measurement Institute at North Ryde.

The analytical methods used mirror those described in USEPA Methods 3050; 200.8; 200.7, 6010, 6020 (for acid digestible  $\text{Cr}_{\text{AD}}$ ) and USEPA Method 3060A (Cr(VI)) with some guidance from Furtmann and Seifert (1990) (USEPA 1994b; USEPA 1994a; USEPA 1996b; USEPA 2007). Limits of reporting (LOR) for the methods are typically 0.5 mg/kg, although detection limits may be significantly lower (0.05-0.10 mg/kg). At these lower detection levels, the error of quantification may be significant (up to 0.1 mg/kg), therefore results in the range below 0.5 mg/kg should be seen as qualitative only.

The acid dissolution method used for the samples allows the measurement of elements which under the most extreme leaching event could be released into the environment. Analysis of the resultant leachate was by inductively coupled plasma – mass spectrometry (ICP-MS). The acid dissolution method uses 1:1 concentrated  $\text{HNO}_3$  and HCl at near boiling point ( $95^\circ\text{C}$ ) as a leachate over a two hour period. This method does not measure inaccessible material locked within siliceous glasses (Goodarzi and Huggins 2005) and which will not be released when subjected to environmental leaching.

$\text{Cr}_{\text{AD}}$  was measured in all samples and these results appear in Table 1. In the coal feeds,  $\text{Cr}_{\text{AD}}$  ranged from 3.6 mg/kg (coal MN, bituminous) to 7.2 mg/kg (coal CL, sub-bituminous). Interestingly this differentiation could not be seen in the earlier results and may indicate chromium containment by alternate species in the differently ranked coals. In the furnace ash and fly ash samples  $\text{Cr}_{\text{AD}}$  varied from a low value of 1.5 mg/kg to a high of 13 mg/kg. As a result of the differing aims of the sample dissolutions, estimated composite  $\text{Cr}_{\text{AD}}$  levels determined in flyash and furnace ash samples (Table 1) are significantly lower than those for total sample chromium ( $\text{Cr}_{\text{total}}$ ) in the physically composited ash samples from the Callide fieldwork which were reported earlier (Morrison et al. 2014).

For comparative purposes both sets of results,  $Cr_{total}$  and  $Cr_{AD}$ , have been included in Table 1 and compared in Figure 2. The consistency of these results is encouraging and suggests that somewhere between 80-90% of the total chromium in the ash samples, probably in the form of impurities in siliceous glasses, is inaccessible to infiltrating leach solutions and is therefore environmentally benign. Both  $Cr_{total}$  and particularly  $Cr_{AD}$  are at low levels when compared to the health based investigation levels for soils containing Cr of 100 mg/kg and therefore should be of low environmental risk (enHealth 2001). There appear to be only small differences between results achieved under air or oxy-fired conditions. Although for the blended coals (CL+BL and CL+MN) and coal CL, both  $Cr_{total}$  and  $Cr_{AD}$  are higher under oxy-fired conditions, this is reversed in the runs with the MN bituminous coal. It is possible that this is due to the recycling of the volatile Cr component during oxy-firing resulting in some fly ash enrichment. The inconsistency with the MN coal tests may be due the burner problems encountered at the time, where very high ash in coal levels occurred following failure of the coal swirler in the burner. The enrichment hypothesis receives some reinforcement from the existence of a relatively consistent pattern appearing to be present where  $Cr_{AD}$  values are higher in the latter part of the flyash collection system (Hoppers E –H) giving a suggestion of some differential enrichment in the smaller particles.

Hexavalent chromium [Cr(VI)] was below the LOR (0.5 mg/kg) for all samples. A further qualitative examination of the results was carried out where a lower detection limit of 0.05 mg/kg was accepted. As stated previously, acceptance of these results is inherent on seeing them as qualitative as the error in the determination is necessarily high.

Using this lower detection limit Cr(VI) was detected (although often at levels an order of magnitude below the LOR of 0.5 mg/kg) in 33 of the 193 samples analysed. Cr(VI) was not detected in any of the coal, bottom ash, rear pass or air heater ash samples, this is not unexpected and is consistent with the previous finding of others (Meij 1994; Goodarzi and Huggins 2005; Stam et al. 2011). In the flyash samples the detected values for Cr(VI) ranged from the lowered detection limit (0.05 mg/kg) to a maximum of 0.30 mg/kg. Table 2 shows the results obtained.

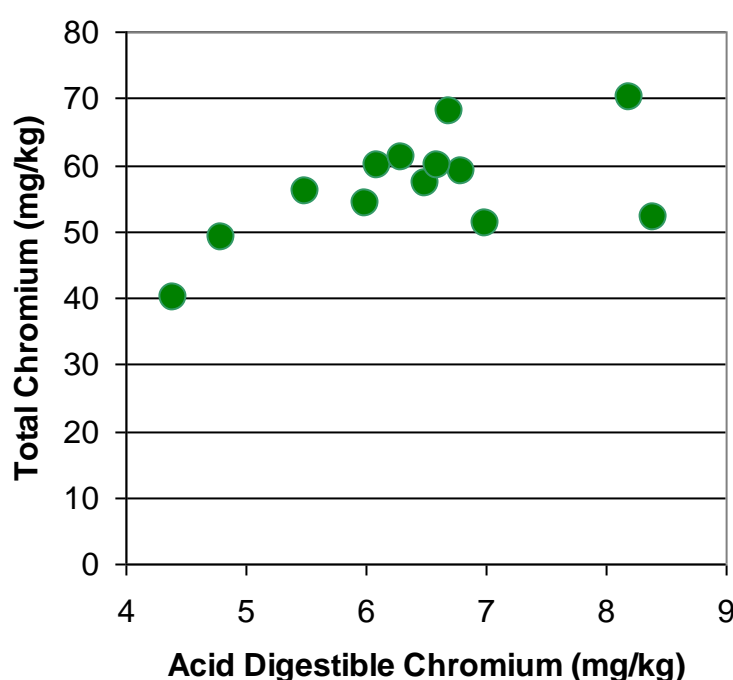


**Figure 2 Comparison of total and acid digestible chromium in composited ash from Callide Oxy-fuel field trials, December 2012.**

Of interest, the Cr(VI) results in Table 2 show that it is predominantly in flyash samples from the later hoppers in the collection train (designated E-H, Figure 3 Callide Field trial report (Morrison et al. 2014)) where Cr(VI) could be detected. This suggests that conversion of the chromium is happening either in only the smallest particles or that the conversion process has some time or temperature dependency, given that the time taken for an individual particle to reach this point would be longer and the temperature would have had the opportunity to decrease to lower levels than for those particles collected in hoppers A-D. It may also be that simply more of the liberated Cr is being deposited in these hoppers as a similar pattern also seems to occur for Cr<sub>AD</sub>.

In the experiment carried out on the 20<sup>th</sup> of December, the burner swirler failed and combustion efficiency was lowered significantly and this resulted in high levels of unburnt carbon in the flyash. This lowered flame effectiveness seems to correspond to increased detection of Cr(VI) in the flyash and may point to mechanisms for formation which deserve further investigation.

### **3.1.5 Application of the chromium results to the Callide Oxy-fuel process**

Levels of environmentally available chromium in the ash samples from the Callide field trials are low (4.4 – 8.4 mg/kg). The environmentally available chromium (determined by an aggressive acid digestion) is 10-15% of the total chromium, which includes chromium isolated within the siliceous glass matrix, this material is not available even in aggressive acid environments and therefore poses no environmental risk.

The carcinogenic hexavalent form of chromium [Cr(VI)] was below the normal limit of reporting of 0.5 mg/kg for this oxidated chromium state. Re-evaluation of these data using a lower detection limit of 0.05 mg/kg (with inherent high errors in quantification) showed that this species was likely present at very low levels in some of the fly ash samples. There seems to be a potential relationship between the presence of Cr(VI) and finer sized fly ash particles given the general increase in Cr levels in the FF collection train.

**Table 1 Results of ash and coal analyses for acid digestible chromium (Cr<sub>AD</sub>) (values are mg/kg)**

SAMPLE DATE	5/12/2012	6/12/2012	7/12/2012	8/12/2012	10/12/2012	11/12/2012	12/12/2012	13/12/2012	16/12/2012	17/12/2012	18/12/2012	19/12/2012	20/12/2012
FIRING CONDITION	OXY	OXY	OXY	AIR	AIR	OXY	OXY	OXY	OXY	OXY	AIR	AIR	OXY
Coal Type	CL	CL	CL+ BL	CL+BL	CL+ MN	CL+MN	CL	CL	CL	CL	CL	MN	MN
			BLEND 1	BLEND 1	BLEND 2	BLEND 2							
Coal	7.1		5.5	5.6	5.6	5.0	6.6	7.2	7.2	6.7	7.8	3.6	
Fabric Filter A	4.0	12.0	4.1	4.7	3.2	9.4	2.3	11.0	5.3	2.6	4.8	8.8	2.7
Fabric Filter B	8.6	5.2	7.6	3.7	4.1	7.6	9.4	7.1	10.0	9.7	6.9	4.2	7.5
Fabric Filter C	7.0	13.0	11.0	4.5	3.3	7.1	11.0	11.0	5.6	6.2	4.7	9.9	8.3
Fabric Filter D	8.3	11.0	6.9	4.2	6.2	7.2	5.8	12.0	9.4	8.0	8.2	8.0	5.5
Fabric Filter E	11	9.0	11.0	5.4	7.7	7.6	9.0	10.0	6.7	11.0	10.0	8.5	5.9
Fabric Filter F	10	10.0	11.0	5.4	9.0	6.4	8.0	7.9	11.0	12.0	8.5	5.9	7.6
Fabric Filter G	11	10.0	11.0	6.2	10.0	7.8	9.8	11.0	9.8	12.0	11.0	8.0	8.6
Fabric Filter H	12	12.0	11.0	4.5	11.0	11.0	11.0	11.0	8.5	13.0	11.0	9.6	8.7
Rear Pass A	3.4	3.2	3.4	3.6	3.1	2.1	2.3	2.8	2.4	3.4	2.6	3.5	4.4
Rear Pass B	3.3	3.4	2.8	3.5	3.2	2.9	2.1	3.3	2.7	3.2	3.4	3.5	3.5
Air Heater A	2.3	2.0	2.6	2.9	2.1	1.5	1.4	1.8	2.9	2.1	2.3	4.0	4.1
Air Heater B	2.6	1.9	1.9	2.9	2.1	1.9	1.5	1.7	2.3	1.8	2.7	4.0	2.9
Furnace Ash	2.6	2.4	2.5	4.2	4.1	2.4	2.3	2.0	2.8	1.7	3.3	5.6	3.3
Overall Combined Ash (mg/kg) (Cr <sub>AD</sub> ) <sup>1</sup>	6.5	8.4	6.8	4.4	4.8	6.7	6.1	8.2	6.6	6.3	6.0	7.0	5.5
Weighted average FF (mg/kg) <sup>1</sup>	7.6	10.1	8.0	4.6	5.2	7.9	7.3	10.0	7.7	7.6	6.9	7.6	6.1
Total Cr (Cr <sub>total</sub> ) (mg/kg) <sup>2</sup>	57	52	59	40	49	68	60	70	60	61	54	51	56

<sup>1</sup> values calculated from standardised mass fractions reporting to individual ash compartments [see Table 3 Morrison *et al.*(2014)]

<sup>2</sup> ash samples physically composited prior to analysis



**Table 2 Results of ash and coal analyses for Cr(VI) (values<sup>1</sup> are µg/kg)<sup>2</sup>**

SAMPLE DATE	5/12/2012	6/12/2012	7/12/2012	8/12/2012	10/12/2012	11/12/2012	12/12/2012	13/12/2012	16/12/2012	17/12/2012	18/12/2012	19/12/2012	20/12/2012
FIRING CONDITION	OXY	OXY	OXY	AIR	AIR	OXY	OXY	OXY	OXY	OXY	AIR	AIR	OXY
Coal Type	CL	CL	CL+ BL	CL+BL	CL+ MN	CL+MN	CL	CL	CL	CL	CL	MN	MN
			BLEND 1	BLEND 1	BLEND 2	BLEND 2							
Coal	<mdl	<mdl	<mdl	<mdl	<mdl	<mdl	<mdl	<mdl	<mdl	<mdl	<mdl	<mdl	
Overall FF UBC%	2.5	1.3	5.2	13.6	7.8	4.5	3.4	1.6	1.3	2.6	5.7	14.2	16.2
Fabric Filter A	<mdl	<mdl	<mdl	<mdl	<mdl	77	<mdl	68	<mdl	<mdl	<mdl	111	<mdl
Fabric Filter B	<mdl	<mdl	<mdl	<mdl	<mdl	<mdl	<mdl	<mdl	<mdl	<mdl	<mdl	<mdl	305
Fabric Filter C	<mdl	<mdl	<mdl	<mdl	<mdl	<mdl	131	60	<mdl	<mdl	<mdl	176	229
Fabric Filter D	<mdl	<mdl	<mdl	<mdl	<mdl	<mdl	<mdl	112	53	<mdl	67	<mdl	55
Fabric Filter E	<mdl	<mdl	<mdl	<mdl	53	<mdl	<mdl	71	<mdl	<mdl	81	<mdl	n.d.
Fabric Filter F	<mdl	<mdl	<mdl	<mdl	<mdl	<mdl	61	<mdl	<mdl	55	<mdl	<mdl	164
Fabric Filter G	59	<mdl	<mdl	<mdl	59	54	67	<mdl	<mdl	60	107	<mdl	149
Fabric Filter H	<mdl	<mdl	<mdl	108	94	107	79	122	<mdl	<mdl	70	81	167
Rear Pass A	<mdl	<mdl	<mdl	<mdl	<mdl	<mdl	<mdl	<mdl	<mdl	<mdl	<mdl	<mdl	<mdl
Rear Pass B	<mdl	<mdl	<mdl	<mdl	<mdl	<mdl	<mdl	<mdl	<mdl	<mdl	<mdl	<mdl	<mdl
Air Heater A	<mdl	<mdl	<mdl	<mdl	<mdl	<mdl	<mdl	<mdl	<mdl	<mdl	<mdl	<mdl	<mdl
Air Heater B	<mdl	<mdl	<mdl	<mdl	<mdl	<mdl	<mdl	<mdl	<mdl	<mdl	<mdl	<mdl	<mdl
Furnace Ash	<mdl	<mdl	<mdl	<mdl	<mdl	<mdl	<mdl	<mdl	<mdl	<mdl	<mdl	<mdl	<mdl

<sup>1</sup>Detection limit lowered to 50 µg/kg ( at this level error bands are large and may exceed ±100 µg/kg)

<sup>2</sup> **Note change to concentration scale** from Table 1. <sup>3</sup> minimum detection limit (mdl)

## 4. ALLOWABLE LEVELS OF TRACE ELEMENTS IN CO<sub>2</sub>

One of the goals of the project was to assess the ultimate trace component concentrations in product CO<sub>2</sub>, and assess the suitability of the CO<sub>2</sub> for various uses (eg, pipeline quality for transport and storage; comparison with food grade CO<sub>2</sub> and whether the product CO<sub>2</sub> would require additional cleaning required to meet food grade standards.

### 4.1 Food grade CO<sub>2</sub>

Although there is guidance on standards for food grade CO<sub>2</sub> for many impurities, there is little direct guidance provided for trace elements, the potential presence of particular species (such as mercury) is acknowledged depending on the source of the feed gas. Typical of the standards set is the following from a working group of the European Industrial Gases Association (EIGA) in conjunction with the Compressed Gases Association of America (CGA) and the International Society of Beverage Technologists (ISBT) to provide guidance on standards for source qualification and specification of bulk carbon dioxide for use in foods and beverages (EIGA 2008).

**Table 3 Limiting characteristics for carbon dioxide for foods and beverages (EIGA 2008)**

Component	Concentration			
Assay	99.90%	v/v		min.
Moisture	50	ppm	v/v	max.
Ammonia	2.5	ppm	v/v	max.
Oxygen	30	ppm	v/v	max.
Oxides of nitrogen (NO/NO <sub>2</sub> )	2.5	ppm	v/v	max.
Non-volatile residue (particulates)	10	ppm	w/w	max.
Non-volatile organics residue (oil and grease)	5	ppm	w/w	max.
Phosphine	0.3	ppm	v/v	Max
Total volatile hydrocarbons (calculated as methane)	50	ppm	v/v	max.of which 20 ppm (v/v) max non-methane hydrocarbons
Acetaldehyde	0.2	ppm	v/v	max.
Benzene	0.02	ppm	v/v	max.
Carbon Monoxide	10	ppm	v/v	max.
Methanol	10	ppm	v/v	max.
Hydrogen Cyanide	0.5	ppm	v/v	Max
Total Sulfur (as S)	0.1	ppm	v/v	max.
Taste and odour in water	No foreign taste and odour			

As can be seen from Table 3 although many (mostly hydrocarbon) components are specified, no specification is included for other trace elements. The EIGA (2008) guidance document suggests a method for calculation of acceptable levels for unlisted compounds which are “yet unknown or undetected in some carbon dioxide source”.

The calculation method suggests using national drinking water standards and the “worst case” assumption that any impurities in the liquid CO<sub>2</sub> are consumed in a beverage product. For the calculation a volume of CO<sub>2</sub> gas of 4.02 L CO<sub>2</sub>(gas)/L<sub>beverage</sub> (8g, liquid CO<sub>2</sub>) is consumed per litre of beverage. The concentration of a substance allowable in the liquid CO<sub>2</sub> is then given by:

$$\text{Concentration in CO}_2 \text{ (mg/Nm}^3\text{)} = [\text{Drinking water guideline value mg/L}]/[4.02/1000 \text{ Nm}^3\text{CO}_2/\text{L}_{\text{beverage}}]$$

Using the National Health and Medical Research Council (NHMRC 2004) and World Health Organisation (WHO 2008) drinking water guidelines a table of acceptable concentrations for the trace elements of interest has been constructed and appears as Table 4.

**Table 4 Calculated maximum acceptable concentrations of elements in produced CO<sub>2</sub> for food use based on NHMRC water guidelines (greyed areas based on MDL)**

Element	Drinking Water Guideline value <sup>1</sup> (mg/L)	Calculated maximum allowable concentration in CO <sub>2</sub> (mg/Nm <sup>3</sup> )	Measured concentration in CPU at Drier Outlet (mg/nm <sup>3</sup> )
Antimony	0.003	0.7	<0.00082
Arsenic	0.007	1.7	<0.0021
Beryllium	0.5 <sup>2</sup>	123	<0.00082
Boron	4	983	<0.0021
Cadmium	0.002	0.5	0.0019
Chromium	0.05	12.3	<0.00082
Cobalt	ng <sup>3</sup>	ng	<0.00082
Copper	2	491	0.0014
Lead	0.01	2.5	<0.00082
Manganese	0.5	123	0.012
Mercury	0.001	0.2	<0.000002
Nickel	0.02	4.9	<0.00082
Selenium	0.01	2.5	<0.0021
Zinc	3	737	0.0076
Chlorine	0.6	147.4	<0.16
Sulfur <sup>4</sup>		0.6	<0.5

<sup>1</sup> all values NHMRC (2004) unless otherwise noted

<sup>2</sup> WHO (2008) <sup>3</sup> ng no guidance value provided <sup>4</sup> EIGA (2008)

The information provided in Table 4 suggests that concentrations of a range of elements measured in the CPU during the field trial program are orders of magnitude lower than possible allowable limits for inclusion in food grade CO<sub>2</sub>, with the exception of sulfur which at 0.5 mg/Nm<sup>3</sup> is close to the limit of 0.6 mg/Nm<sup>3</sup>. However as the hydrocarbons, oxides of nitrogen and many other species given in Table 3 were not measured during the field trial, it is not possible to unequivocally state that the product CO<sub>2</sub> would be acceptable, until this analysis has occurred.

## 4.2 Pipeline Grade CO<sub>2</sub>

Safe, reliable, and cost effective transport of the CO<sub>2</sub> by pipeline requires that the CO<sub>2</sub> stream meet certain specifications. Impurities in the CO<sub>2</sub> stream can impact the transport capacity of the pipeline, the potential for micro-fractures in the pipeline, and other safety and operational considerations to mitigate against substantial leakage, rupture, or incident (UNIDO 2011). It should be noted that this specification is for gasification derived CO<sub>2</sub>, thus the inclusion of H<sub>2</sub>S and exclusion of SO<sub>2</sub> which may be more relevant in a specification relating to Oxyfuel processing.

Pipeline specifications exist for CO<sub>2</sub> use in other applications such as enhanced oil recovery where the more stringent standards required in the food industry are not required, its is expected that these specifications would be acceptable were the CO<sub>2</sub> to be used for CCS. A typical specification for pipeline quality CO<sub>2</sub> appears in Table 5. A comprehensive review of pipeline specifications carried out by the Oxy-fuel Working Group, this review which includes other parameters and species is available online<sup>1</sup>.

**Table 5 Typical pipeline CO<sub>2</sub> specification for enhanced oil recovery (UNIDO 2011).**

Component	Specification (maximums)	Reason for inclusion
CO <sub>2</sub>	95%	MMP <sup>1</sup>
Nitrogen	4%	MMP <sup>1</sup>
Hydrocarbons	5%	MMP <sup>1</sup>
Water	480 mg/m <sup>3</sup>	Corrosion
Oxygen	10 ppm	Corrosion
H <sub>2</sub> S	10-200 ppm	Safety
Glycol	0.04 mL/m <sup>3</sup>	Operations
Temperature	65°C	Material integrity

<sup>1</sup> Maintenance of minimum miscible pressure

Like the discussion on food grade CO<sub>2</sub> no specification seems to exist for a range of elements (particularly metals) in the produced CO<sub>2</sub> for pipeline use, although given the wide margin with which the CPU product exceeds the allowable limits for the food grade material it is unlikely, at least for those elements, that any difficulties with its use should be encountered. It has been suggested (Wall *pers comm*) that a likely source of limitations on use may be from

<sup>1</sup>

[http://www.google.com.au/url?sa=t&rct=j&q=&esrc=s&source=web&cd=1&ved=0CB4QFjAA&url=http%3A%2F%2Fwww.newcastle.edu.au%2FResources%2FProjects%2FAsia%2520Pacific%2520Partnership%2520Oxy-fuel%2520Working%2520Group%2FGuidelines-and-regulations-for-oxyfuel.doc&ei=4VCqU6jyDofHkAXx84B4&usq=AFQjCNGUAkam6B0MFq2zZhWZ\\_T3Edpknw&sig2=hOslVAUYd0spDwWAYyG8hQ](http://www.google.com.au/url?sa=t&rct=j&q=&esrc=s&source=web&cd=1&ved=0CB4QFjAA&url=http%3A%2F%2Fwww.newcastle.edu.au%2FResources%2FProjects%2FAsia%2520Pacific%2520Partnership%2520Oxy-fuel%2520Working%2520Group%2FGuidelines-and-regulations-for-oxyfuel.doc&ei=4VCqU6jyDofHkAXx84B4&usq=AFQjCNGUAkam6B0MFq2zZhWZ_T3Edpknw&sig2=hOslVAUYd0spDwWAYyG8hQ)

concentrations of oxides of nitrogen which were not measured during the present study on the CO<sub>2</sub> processing unit.

#### ***4.3 Implications of CO<sub>2</sub> quality for the Callide Oxy-fuel process***

The quality of the produced CO<sub>2</sub> for a wide range of elements has been assessed against a calculated value for potential use in the food industry. This standard is much more stringent than that required for pipeline quality for use in enhanced oil recovery. For the elements measured during the field trial all concentration values in the CO<sub>2</sub> produced by the CPU were orders of magnitude lower than the levels which might be required for use in the beverage industry, except for potentially sulfur for which the MDL is close to the allowable limit of 0.6 mg/Nm<sup>3</sup>. However, the food quality specifications include a number of elements and compounds (eg, hydrocarbons, oxides of nitrogen and water) which require further testing and their presence or concentration may preclude this use.

## 5. PREDICTIVE METHODS FOR MERCURY CAPTURE DETERMINATION USING iPOG

The United Nations Environment Program (UNEP) has a Coal Mercury Partnership which has promoted the development of a Process Optimization Guidance document, or POG, which can be used to predict the effects of coal properties, power station design and operating conditions on mercury emissions. The POG includes a decision tree which allows operators of coal-fired power plants to examine and assess Hg control options, whether as a co-benefit from other air pollution control devices or specific Hg emission control strategies.

The **iPOG**<sup>2</sup> develops the POG's decision tree by providing quantitative estimates of Hg emissions in a software package that predicts Hg emission rates from utility gas cleaning systems fired with any coal or coal blend, given a few coal properties, the gas cleaning configuration, selected firing and gas cleaning conditions, and an assortment of Hg control technologies. It predicts the Hg emission reductions for the most common Hg controls, including systems with only particle collection devices (PCDs), and with ESP/FGD and SCR/ESP/FGD combinations. It also predicts Hg removals for injection of conventional carbon sorbents, brominated carbon sorbents, and halogenation agents, and estimates the Hg removals for different coal pre-treatments. The iPOG documentation (Niksa 2011) suggest that these estimates should be accurate enough to enable users to rank-order a broad assortment of options according to the extent of Hg reductions sort and the suitability / practicality of the options for existing gas cleaning configurations. Here we use iPOG to compare mercury measurements from the Callide OxyFuel Plant with predictions based on iPOG. Some of the following discussion has previously been presented in a somewhat different form in the Final Report for ACARP Project C19009 (Nelson and Malfroy 2014).

### 5.1 Inputs

One of the aims in developing the iPOG was to keep it simple and as will be examined in this section this is both an advantage and limitation of the software. As can be seen from Table 6, most of iPOG's data inputs are variables that are commonly available for combustion / emission studies. In the absence of facility -specific data, iPOG provides default values.

### 5.2 Outputs

The iPOG's output is presented in a flow diagram which shows the estimated Hg input to the furnace and the removal rate and speciation of mercury through the furnace, air pre-heater (APH) and APCDS (SCR, PCD, SDA, WFGD). An example of the iPOG output is shown in Figure 3. In this simple case, it is estimated that 78.4% of the mercury is removed with bottom ash from the boiler and with flyash from the fabric filters. The remainder exits the stack, dominantly (95%) as oxidised Hg. At each Hg removal point, the iPOG provides Hg rates in g/h with uncertainty estimates and the fraction of Hg as Hg<sup>2+</sup>.

---

<sup>2</sup>[http://www.unep.org/hazardoussubstances/Portals/9/Mercury/Documents/coal/iPOG\\_v10\\_UserGuide.pdf](http://www.unep.org/hazardoussubstances/Portals/9/Mercury/Documents/coal/iPOG_v10_UserGuide.pdf)

**Table 6: iPOG data inputs**

<b>IPOG data entry window</b>	<b>Variables</b>	<b>Comment</b>
Single coal properties	Moisture (%), ash (%), sulfur (%), chlorine (%), mercury (ppmw) Higher heating value (J/g),	Coal types can be saved
Coal blend properties	Blend percentages of single coal data	Blend types can be saved
Furnace conditions	Furnace rating (MWe), Load (%), LOI (%), Bottom ash (%), Furnace Exit O <sub>2</sub> (%), NO <sub>x</sub> (ppm)	LOI – Loss on ignition as weight loss % after oxidation of flyash.  NO <sub>x</sub> only entered if SCR in use
Post combustion controls	ESPC only, FF only, ESPC +WFGD, SCR +ESPC+WFGD	User enters control efficiencies for APCDs in use
Mercury controls	Inherent only	Based on Chlorine, ash, LOI etc.
	Coal washing, float/sink, blending	User cannot enter efficiencies of these measures
	Halogen use	Chlorine or bromine rate. Injection location (coal/furnace, before /after APH)
	Sorbents (ACI)	Treated or Untreated ACI Injection location
Mercury control parameters	Halogen load rate Sorbent load rate	

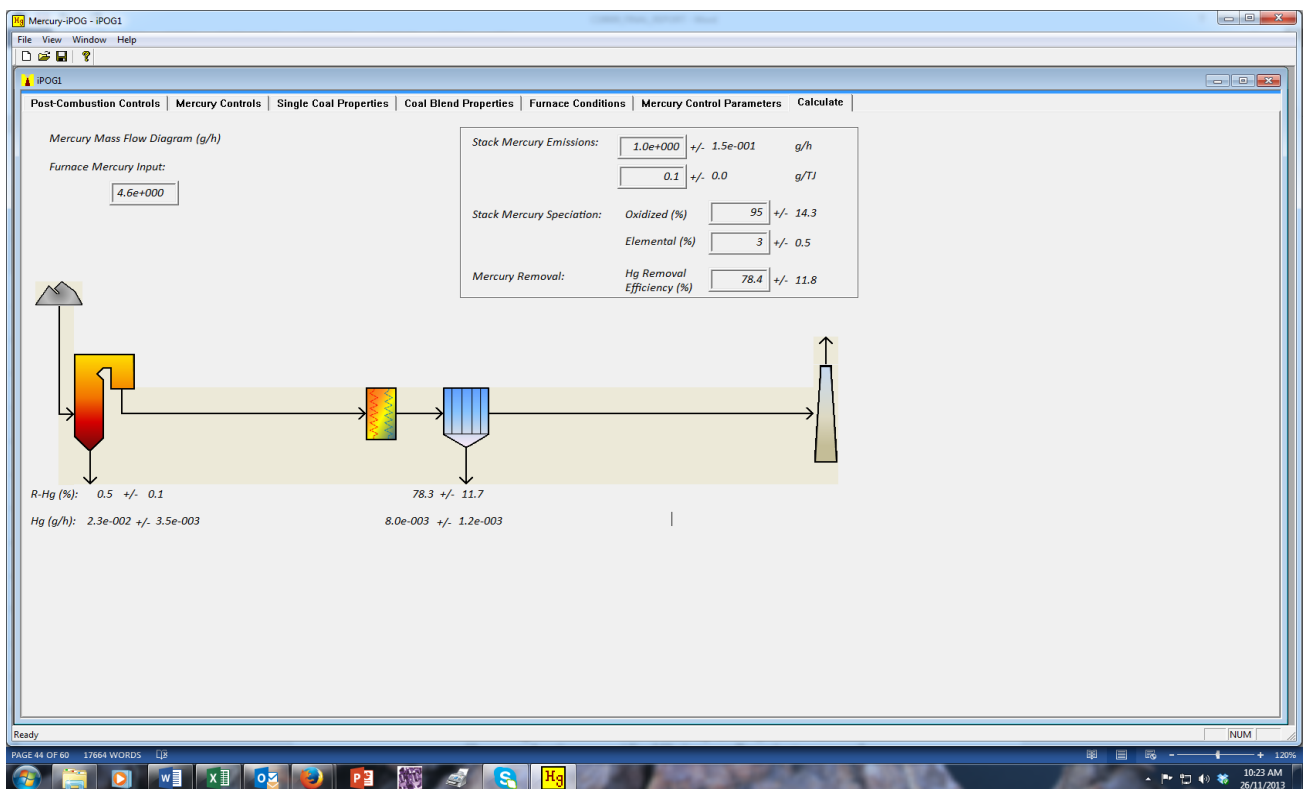


Figure 3: An example of iPOG’s output screen

### 5.3 Uses of iPOG

The data requirements to run iPOG are modest and hence scenarios are quick and easy to evaluate. The iPOG Users’ Guide (Niska 2011) discusses a number of possible uses for the iPOG, which include:

- Running “what if” scenarios to achieve different levels of Hg emission reductions, given coal supply and existing plant configuration constraints.
- Estimating how changes to existing APCDS might affect mercury emissions.
- Estimating how firing conditions, excess oxygen ( $\text{O}_2$ ), LOI, for example, might affect mercury emissions.
- Evaluating future coal supplies and possible blending options.
- Estimating the oxidation state of mercury in the system as this influences Hg removal options, as oxidised Hg is generally easier to remove than elemental Hg.

### 5.4 iPOG Limitations

The iPOG Users’ Guide (Niksa 2011) discusses a number of limitations with the software which are summarised here:

The iPOG estimates are, for the most part, based on regressions of field test data directed by the National Energy Technology Laboratory of the US Dept. of Energy, rather than on validated chemical reaction mechanisms. Notwithstanding the extensive nature of the field tests and careful data quality control, the User Guide cautions that estimates from iPOG are no more accurate than the qualified measurement uncertainties, which are estimated to be at 10 – 15 % of the total Hg inventory in each test.



In order to keep the data requirements manageable and the software “user friendly” for a broad range of potential users, rather than useful to a fewer number of technical specialists, the iPOG does not include state of the art mechanistic descriptions of mercury behaviour. The iPOG documentation notes that *“Trade-offs were deliberately made to eliminate all but the most basic input requirements at the expense of quantitative accuracy for any particular utility gas cleaning system. Obviously, these trade-offs limit how the estimates from the iPOG should be used.”*

Due to the requirement to keep the iPOG simple, all but the essential process characteristics were omitted from the input data requirements meaning it cannot depict the distinctive features of particular gas cleaning systems. For example, users do not specify the temperatures of their PM control devices, which is known to be an important variable in Hg removal. In Activated Carbon Injection (ACI) applications, iPOG does not account for the variable performance of different carbon sorbents, due to differences in preparation techniques, loadings, and surface areas. Also importantly, the interference of sulfur trioxide on the capture of Hg by unburned carbon in ash and on carbon sorbents is not accounted for in the iPOG estimates. It is noted also that Br is not included in the inputs although the effects of Br on Hg capture are well known. In many cases the Cl and Br contents are related, and the inclusion of Cl in the iPOG input parameters may account for these effects.

Design specifications of SCR systems, which can be as important as halogen concentrations in the oxidation of Hg across SCRs, are not included in iPOG, due to technical and sometimes propriety.

iPOG does not account for the possibility that oxidised Hg captured in WFGD systems may be re-emitted as elemental Hg depending on the chemistry of the scrubber solution. *“Consequently, iPOG users should realize that the relatively high Hg removals estimated for cleaning systems with WFGDs will represent significant over-predictions for the unusual situations where re-emission comes into play.”*

iPOG does not include cost estimates, although these would provide relevant, useful information to financial decision making.

## 5.5 Application of iPOG to the Callide OxyFuel Plant data

As noted above, the iPOG’s Hg emission estimates are based primarily on regression equations developed from emission data gained from an extensive campaign in the USA. Australian bituminous coals are different to bituminous coals in the US with respect to a number of parameters, in addition to Hg, which are important in the speciation and collection of Hg. Table 7 indicates that Australian coals tend to have lower chlorine (as well as lower Hg concentrations) and higher ash concentrations than US bituminous coals

**Table 7: Characteristics of US and Australian bituminous coals**

		Ash %	Sulfur %	Chlorine %	Mercury ppmw	HHV MJ/kg
<b>iPOG default coal</b>	<b>Low S bituminous</b>	7	1.8	0.107	0.12	31.5
	<b>High S bituminous</b>	12.1	4.4	0.054	0.17	20.4
<b>Indicative Aust. bituminous</b>		20- 26	0.3 - 0.6	0.02 - 0.04	0.02 - 0.04	22 26

iPOG calculations were made for the measurements from at Callide in 2012. Table 8 presents input data used for the model and observed results for mercury speciation and capture in the particle collection devices at Callide.

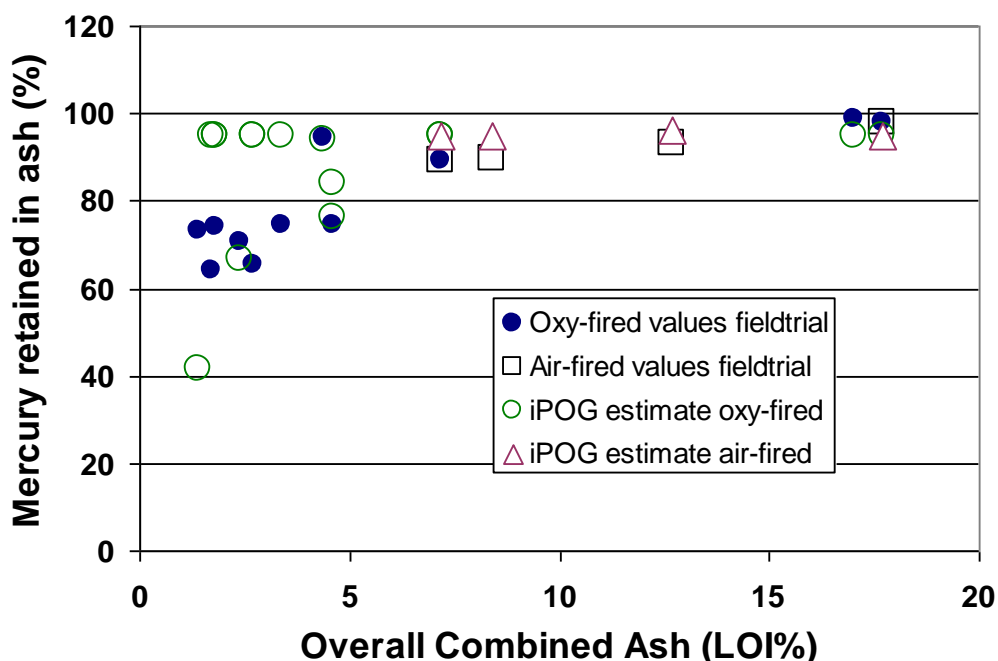


Figure 4: Mercury retained in ash (%) as a function carbon in ash (LOI, %); measurements and predictions using iPOG for air and oxy-fired conditions

Calculations with iPOG and examination of the results of the measurement campaign demonstrated that the removal of mercury in the fabric filters employed at Callide was highly dependent on the amounts of carbon retained in the ash. International experience with mercury reduction in ESPs and especially FFs accords with this observation. Figure 4 presents data for mercury retained in ash as a function of carbon in ash based on measurements and iPOG predictions.

### 5.6 Implications of the iPOG modelling for the Callide Oxy-fuel process

The measured data presented in Figure 4 show that if carbon in ash exceeds ~5%, greater than 90% of the mercury is captured in the fabric filters. For lower levels of carbon in ash mercury captured reduces to 60-80%. iPOG calculations reproduce these results with reasonable precision for air-fired conditions. Agreement for oxy-fired conditions is poorer for some data sets (particularly for LOI less than 5%), which may be due to the source of the data used to develop iPOG in which case the regression does not work as well. This US data did not include any oxy-combustion plants, and the properties of some of the coal blends used at Callide may have fallen outside the range of coals used in the iPOG development

Overall a conclusion that can be drawn from these data and the calculations is that substantial mercury can be removed from the gas stream by the carbon present in the ash. A consequence is that for some operating conditions at Callide most of the mercury will not be transported to the CPU but will require management through the ash stream. It's possible that at larger scale and in new build plants that higher combustion efficiencies will reduce carbon in ash to lower levels and that increasing proportions of mercury from the fired coal will be transported to the CPU.

**Table 8: Input data for iPOG calculations for the Callide OxyFuel Plant (values in bold taken from previous day when unavailable)**

<sup>1</sup> as received    <sup>2</sup> During testing in December 2012 the unit was limited to a nominal 24 MWe due to cooling water temperature limitations on the Air

SAMPLE DATE	5/12/12	6/12/12	7/12/12	8/12/12	8/12/12	10/12/12	11/12/12	12/12/12	13/12/12	14/12/12	16/12/12	17/12/12	18/12/12	19/12/12	20/12/12
FIRING CONDITION	OXY	OXY	OXY	OXY	AIR	AIR	OXY	OXY	OXY	OXY	OXY	OXY	AIR	AIR	OXY
Coal Type	CL	CL	CL	CL+ BL	CL+BL	CL+ MN	CL+MN	CL	CL	CL	CL	CL	CL	MN	MN
			BLEND1	BLEND1	BLEND1	BLEND2	BLEND2								
Moisture (%) <sup>1</sup>	13	<b>13</b>	11.5	12.7	12.7	11.8	12.5	13.5	12.8	12.2	13.3	16	17.1	5.8	<b>5.8</b>
Ash (%) <sup>1</sup>	22.6	<b>22.6</b>	18.9	20.8	20.8	24.8	23.7	25.6	24.2	25.8	22.8	22.2	23.4	23.9	<b>23.9</b>
Sulfur(%) <sup>1</sup>	0.2	<b>0.2</b>	0.27	0.28	0.28	0.26	0.26	0.22	0.22	0.2	0.24	0.2	0.21	0.43	<b>0.43</b>
Chlorine (%) <sup>1</sup>	0.02	<b>0.02</b>	0.04	0.04	0.04	0.04	0.04	0.02	0.01	0.02	0.01	<b>0.01</b>	<b>0.01</b>	0.02	<b>0.02</b>
Coal Hg (ppmw)	0.0314	<b>0.0314</b>	0.0294	<b>0.0294</b>	0.0326	0.034	0.0284	0.0329	0.0347	<b>0.0347</b>	0.0318	0.0312	0.0339	0.0229	<b>0.0229</b>
Gross Calorific Value (J/g) <sup>1</sup>	18910	<b>18910</b>	21910	20590	20590	19040	19040	17750	17970	18050	18630	18030	17280	23430	<b>23430</b>
Furnace rating (MWe)	30	30	30	30	30	30	30	30	30	30	30	30	30	30	30
Furnace Load (%) <sup>2</sup>	0.84	0.81	0.89	0.89	0.83	0.80	0.82	0.80	0.81	0.81	0.80	0.80	0.79	0.80	0.84
Overall Combined Ash (LOI%)	2.4	1.4	4.6	<b>4.6</b>	12.7	8.4	4.4	3.4	1.8	<b>1.8</b>	1.7	2.7	7.2	17.7 <sup>3</sup>	17.0 <sup>3</sup>
Bottom Ash %	15.0	15.0	15.0	15.0	15.0	15.0	15.0	15.0	15.0	15.0	15.0	15.0	15.0	15.0	15.0
Particle Capture Efficiency	99.4	<b>99.4</b>	99.2	<b>99.2</b>	98.5	98.4	99.4	99.5	99.3	<b>99.3</b>	<b>99.3</b>	99.4	98.0	98.0	<b>98.0</b>
Economiser Oxygen (based on 5% air egress to stack)	4.4	4.4	5.3	5.1	4.5	4.3	4.8	4.7	4.4	4.8	5.1	4.7	4.3	4.1	3.9
NOX (ppm)	681	656	696	632	449	452	769	747	713	700	839	789	505	377	533

Separation Units, for consistency all testing (air-fired and oxy-fired) were carried out at a nominal 24 MWe

<sup>3</sup> carbon in ash results during these tests was abnormally high due to the failure of the coal swirler in the burner tube

## 6. SUPPORTING EXPERIMENTAL PROGRAMME

To aid interpretation of the results from the oxy-fuel field trials a large drop tube furnace was utilised to combust small amounts of coal in controlled atmospheres to simulate one aspect of oxyfuel combustion,  $O_2/CO_2$  for oxyfiring compared to  $O_2/N_2$  for airfiring (Figure 5).

It is recognised that this is a simplification of the combustion system and that other relevant differences between oxyfiring and airfiring include higher concentrations of impurity gases such as  $SO_x$  and  $NO_x$  as well as trace element gases and water vapour may well modify trace element behaviour. For example, the differing proportions of recycled gases will vary the levels of these components, soluble gases containing trace elements may be removed to the recycle stream during gas cleaning and water removal; in fact, these effects are already suggested at Callide for Cr (see 3.1.4). Also differing levels of unburnt carbon (oxyfiring often being lower), which was not measured in the current program, will also influence trace element levels and speciation.

### 6.1 Experimental Equipment

The drop tube furnace (Labec, Model VTHTF-130/11-3) had three heating zones and operated to a maximum of  $1100^\circ\text{C}$  (Figure 6). The gases and coal samples were introduced into the DTF through a custom inlet and into a quartz tube (2 m length; wall 5 mm; 50 mm I.D.).



Figure 5 Drop tube furnace used in experimental program.

Injected coal particles passed through the 1.2 metre straight heated flight path and exited the quartz tube via a custom outlet to be collected within a Micro-Orifice Uniform Deposit Impactor (MOUDI), multi-stage impactor, (MSP Corporation, Model 100) (Marple et al. 1991). The impactor fractionated the sample (based on a 50% cut size) into ten size fractions <10, 10, 5.6, 3.2, 1.8, 1.0, 0.56, 0.32, 0.18  $\mu\text{m}$  with a final stage a filter intercepting particles <0.18  $\mu\text{m}$ . Size fractions were collected on pre-weighed stretched Teflon substrates (Pall, Model Teflo 47 mm O.D. x 2.0  $\mu\text{m}$  pore size).

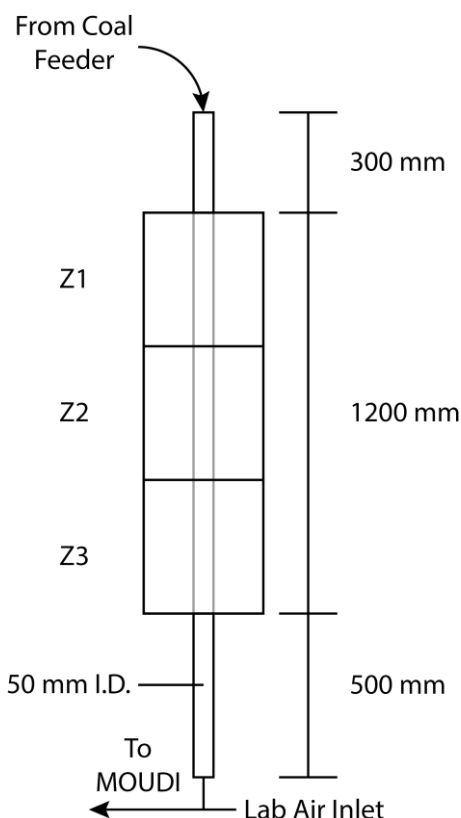


**Figure 6 Schematic diagram of the drop tube furnace showing dimensions of furnace heating zones (Z1-Z3)**

## 6.2 Gas atmospheres

Gas mixtures were created using instrument grade air, high purity  $\text{O}_2$  and food grade  $\text{CO}_2$  controlled by electronic mass flow controllers. Flow for the experiments was controlled at 3 L/min and this was independently validated using a bubble flow meter on the outlet side of the flow controllers. Compositions for the air-fired and oxy-fired conditions were respectively, 100% air and 20%  $\text{O}_2$ / 80%  $\text{CO}_2$ . Residence time for combustion gas in the furnace, assuming plug flow, would be ~15 seconds.

## 6.3 Coal feed

A custom built, vibrating, fluidized bed coal feeder was developed to introduce coal into the DTF (Figure 7). Gas mixtures from the flow controllers were used as the fluidizing gas. Gases entered the base of the feeder and through a stainless steel sintered disc acting as a distributor (Porvair Filtration Group; 2 mm thick; average pore size of 1  $\mu\text{m}$ ). The fluidizing gas was deflected from entering the sintered disc directly to prevent channelling in the coal sample

directly above the gas inlet. The fluidizing gas passed through the disc and escaped the feeder through a 3 mm I.D. outlet tube; in the process small amounts of the milled coal were entrained in the fluidizing gas. The gases and entrained coal were subsequently introduced into the inlet of the DTF via a short length of ¼" Teflon tubing. The entire feeder was fixed to a chemical retort stand upon which was mounted a vibrator (Oli Model MVE 21M); vibrations assisted in disrupting channelling and improving sample entrainment. Additionally, manually actuated rapping was occasionally employed to supplement the vibrator. Coal feedrate showed some variation and was maintained between 0.2 -0.5 g/min.

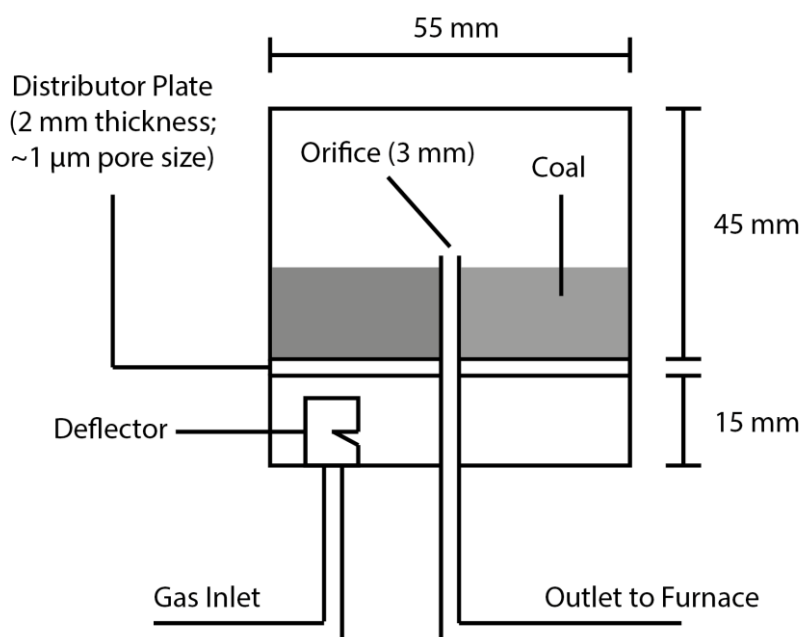


**Figure 7 Schematic diagram of fluidized feeder developed for the drop tube furnace.**

#### **6.4 Feed coal size and analyses**

Three coals sampled from the Callide A Plant during the 2012 Oxy-fuel Field trials (Morrison et al. 2014) were used in the laboratory under conditions simulating oxy and air firing. These coals were designated CL,BL and MN and a sub-bituminous coal (CL), a blend of sub-bituminous and semi-anthracite coals (BL) and a bituminous coal (MN). The coals were collected on the 12<sup>th</sup> (CL), 8<sup>th</sup> (BL) and 19<sup>th</sup> (MN), December 2012 and were analysed for COSPL as part of the field trial program and those analyses are reproduced as Table 9.

The coal samples were sized by sieving at 125 µm and the experiments were carried out using the -125 µm fraction.

**Table 9 Coal analyses (supplied by COSPL)**

Major oxides as % of ash				Trace elements as mg/kg (dry)			
Sample Date	8/12/12	12/12/12	19/12/12	Sample Date	8/12/12	12/12/12	19/12/12
Firing Condition	AIR	OXY	AIR	Firing Condition	AIR	OXY	AIR
Coal Type	CL+BL	CL	MN	Coal Type	BL	CL	MN
	BLEND1			(%)	BLEND1		
Total Moisture (%) <sup>1</sup>	12.7	13.5	5.8	SiO <sub>2</sub>	53.20	56.2	64.0
Ash (%) <sup>1</sup>	20.8	25.6	23.9	Al <sub>2</sub> O <sub>3</sub>	30.1	30.9	23.6
Volatile Matter (%) <sup>1</sup>	17.2	20.4	27.9	Fe <sub>2</sub> O <sub>3</sub>	8.5	7.2	4.97
Fixed Carbon (%) <sup>1</sup>	49.3	40.6	42.4	CaO	1.47	0.94	0.60
Fuel Ratio (FC/VM) <sup>1</sup>	2.86	1.99	1.52	MgO	0.9	0.73	0.83
Total Sulfur(%) <sup>1</sup>	0.28	0.22	0.43	Na <sub>2</sub> O	0.2	0.17	0.22
Chlorine (%) <sup>1</sup>	0.04	0.02	0.02	K <sub>2</sub> O	1.29	0.20	2.31
Gross Calorific Value (MJ/kg) <sup>1</sup>	20.59	17.75	23.43	TiO <sub>2</sub>	1.8	1.83	1.01
HGI <sup>2</sup>	85	80	50	Mn <sub>3</sub> O <sub>4</sub>	0.17	0.18	0.07
				P <sub>2</sub> O <sub>5</sub>	0.43	0.04	0.96
Carbon (%) <sup>3</sup>	81.49	75.28	n.a.	SO <sub>3</sub>	1.19	1.06	0.32
Hydrogen (%) <sup>3</sup>	4.04	3.73	5.59	SrO	0.03	nd*	0.18
Nitrogen (%) <sup>3</sup>	1.4	1.11	2.76	BaO	0.13	0.03	0.37
Sulfur (%) <sup>3</sup>	0.42	0.43	0.65	ZnO	nd*	nd*	nd*
Oxygen (%) <sup>3</sup>	12.65	19.45	4.09	V <sub>2</sub> O <sub>5</sub>	0.03	0.03	0.03

\*nd not detected

<sup>1</sup> as received

<sup>2</sup> Hardgrove Grindability Index

<sup>3</sup> dry ash free

## **6.5 Analysis of MOUDI substrates retaining sized coal ash samples**

The sized ash samples collected on the MOUDI Teflon substrate during the experiments were analysed by the Australian Nuclear Science and Technology Organisation (ANSTO) using a multi-element ion beam analytical (IBA) technique. The IBA technique is well suited to elemental analysis of the substrates as it is non-destructive and can detect a broad range of elements at low minimum detection limits and sample sizes (picograms in micrograms of sample). The use of two IBA techniques, particle induced X-ray and gamma ray emission (PIXE and PIGE), allowed the determination of the following commonly occurring elements; Na, Al, Si, P, S, Cl, K, Ca, Ti, V, Cr, Mn, Fe, Co, Ni, Cu, Zn, Br and Pb. (Cohen et al. 1996; Cohen et al. 2004). IBA analysis was carried out using a 10 mm beam size, located centrally on the Teflon substrate.

IBA of the MOUDI samples has an artefact due to the non-uniform distribution of the combusted material (Appendix A), while the chemistry of the area analysed is internally consistent, as a result of the non-uniform material distribution across the filter surface it is not possible to easily extrapolate the data from the area analysed to reconstruct a mass for the entire substrate (Stelcer et al. 2011).

IBA analyses for the sized substrate samples generated appear as Appendix A. The Ion Beam analyses was blank corrected and where these blank corrected values were determined as non-detects, a value equal to half the minimum detection limit (MDL) was substituted to allow ongoing analysis. The IBA data from the first substrate stage was not used in subsequent examinations as no selective sizing takes place in this material.

## **6.6 Results and discussion of drop tube experiments**

As discussed previously the distribution of trace elements from fuel combustion is critical to both its effective furnace operation and environmental performance. The distribution is not only dependent upon the high temperature transformations of the elements themselves but also the physical and chemical make up of the resultant combusted particles (Helble 1994).

It has been previously pointed out that while most of the mass of ash produced following pulverized fuel combustion of coal is in the larger sizes (1-20  $\mu\text{m}$ ), the particles in the submicron size ranges, which constitute often only 1% of the mass, contribute most of the available surface area (Haynes et al. 1982). The mass concentrations of these small particles have been shown to increase with increasing furnace temperature but not  $\text{CO}_2$  concentration (Jia and Lighty 2012), which is encouraging for the oxy-fuel combustion technology. It is these small particles which provide initial sites for condensation of volatile trace elements, but these condensed trace elements can in turn be scavenged by the larger particles and subsequently redeposited (Haynes et al. 1982). Others have commented on the low capture efficiencies for these smaller particles, particles which in turn can transport an increased proportion of some volatile trace elements (Bool and Helble 1995; Querol et al. 1995).

The distribution of trace elements amongst the ash components in conventional pulverized fuel combustion has been extensively studied and reviewed ((Helble 1994; Bool and Helble 1995; Xu et al. 2003; Huang et al. 2004). The current work seeks to extend the limited work on trace element behaviour in oxy-fired atmospheres (Chen et al. 2012; Wang et al. 2012; Kazanc et al. 2013; Maffei et al. 2013; Song et al. 2013; Zhao et al. 2013; Sporl et al. 2014)



by looking in the laboratory setting, specifically at the example of some of the coals used in the December 2012 Oxy-fired field trials at Callide.

### 6.6.1 Enrichment Factor

To attempt to better understand the behaviour of the elements studied in the ash following combustion in the drop tube furnace, the elemental analysis was normalized with respect to the refractory (non-volatile) aluminium component. This has been done with some success previously in drop tube studies using conventional combustion gases (Querol et al. 1995). The enrichment factor (EF) then becomes:


$$EF = ([X]_{\text{ash}}/[Al]_{\text{ash}})/([X]_{\text{coal}}/[Al]_{\text{coal}}) \quad (1)$$

where  $[X]_{\text{ash}}$  and  $[X]_{\text{coal}}$  are the concentrations of element X in the ash and coal respectively, and  $[Al]_{\text{ash}}$  and  $[Al]_{\text{coal}}$  are the corresponding aluminium contents in the ash and coal. The assumption is made in the calculation of EF that prior to combustion the coal analysis is invariant across the size fractions. As discussed previously, given that during combustion there are major decreases in particle size, this is probably a reasonable approximation which can be tested to some extent by looking at the effect amongst two such refractory elements such as both Al and Si.

Given that the analysis of the coal and the ash have been carried out using very different technologies and the concentrations of some elements analysed in both the coal and ash are small it is unsurprising that the inherent error and scatter occurs. More importantly it is the shape of the curves and magnitude of the change observed when plotted against particle size, which give clues to the behaviour of the elements being examined rather than the absolute values which maybe driven up or down relatively by small changes to the input coal analysis. Plots for all elements analysed by both PIXIE and in the coals are given in Figure 8 to Figure 23 and a qualitative description is given for the behaviour of the elements in Table 11 with an indication as to whether differences between the air and oxy-fired conditions are apparent.

Elements have been grouped according to the scheme proposed by Meiji (1994; 2007) which is reproduced as Table 10 (elements in **bold** are in both the coal and ash analytical suite).

**Table 10 Categorisation of elements based on volatility behaviour (after Meiji, 1994, 2007)**

<div style="writing-mode: vertical-rl; transform: rotate(180deg);">Increasing volatility</div> 	Class	Element	Description	Outcome
	I	<b>Al, Ca, Ce, Cs, Eu, Fe, Hf, K, La, Mg, Sc, Sm, Si, Sr, Th, Ti</b>	Not volatile	Distributed between bottom ash and flyash
	IIa	<b>Be, Co, Cu, Ni, P, U, V</b> and W	Volatile in boiler, significant condensation in particle collection device (PCD) on flyash	Enriched in flyash and depleted in bottom ash when compared to input coal.
	IIb	<b>Ba, Cr, Mn, Na</b> and Rb		
	IIc	<b>As, Cd, Ge, Mo, Pb, Sb, Tl</b> and <b>Zn</b>		
	III	<b>B, Br, C, Cl, F, Hg, I, N, S</b> and <b>Se</b>	Volatile: some to hardly any condensation on ash particles in PCD	Lowest boiling point elements emitted fully in vapour phase and not enriched in flyash

The following figures of EF as a function of size all follow a similar format with the top three being the experiments using a simulated oxy-firing gas composition, coal types CL,BL (Blend 1) and MN, with the following row of three diagrams being for the air-fired condition.

## 6.6.2 GROUP I elements (Si, Ca, Ti, Fe, K)

Figure 8 EF of silicon in coal ash as a function of size <10  $\mu\text{m}$ .

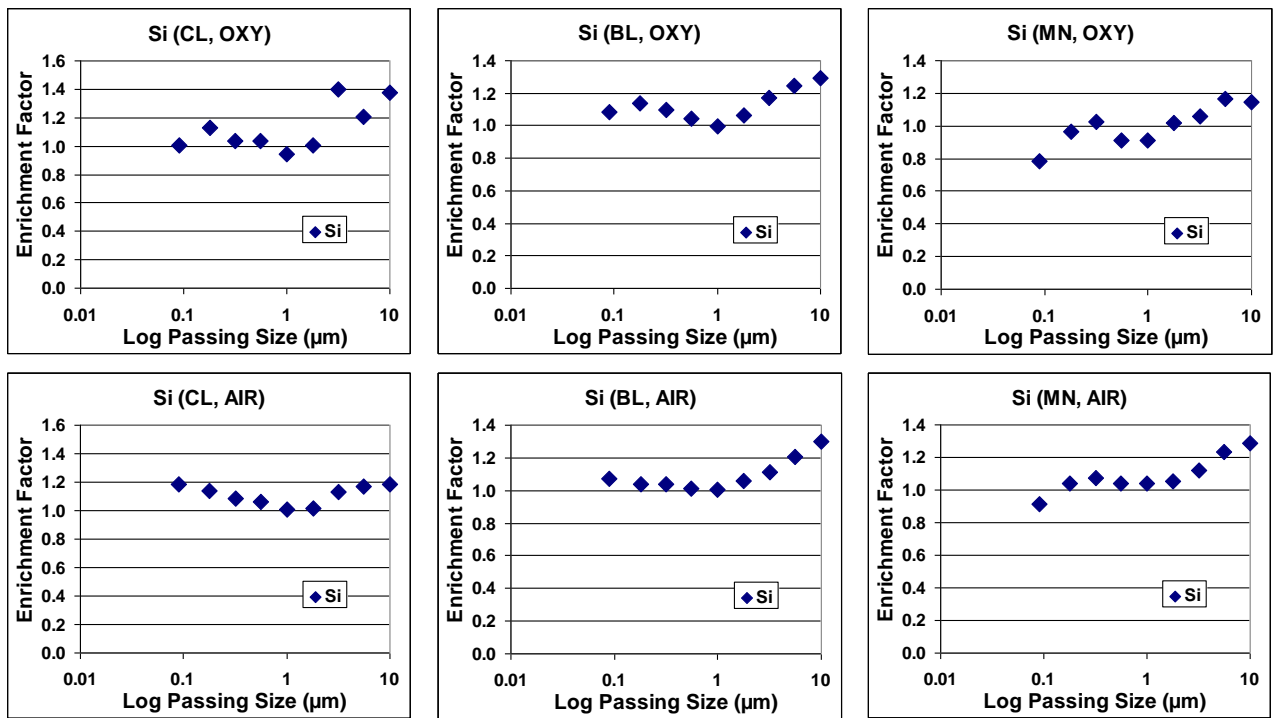


Figure 9 EF of calcium in coal ash as a function of size <10  $\mu\text{m}$ .

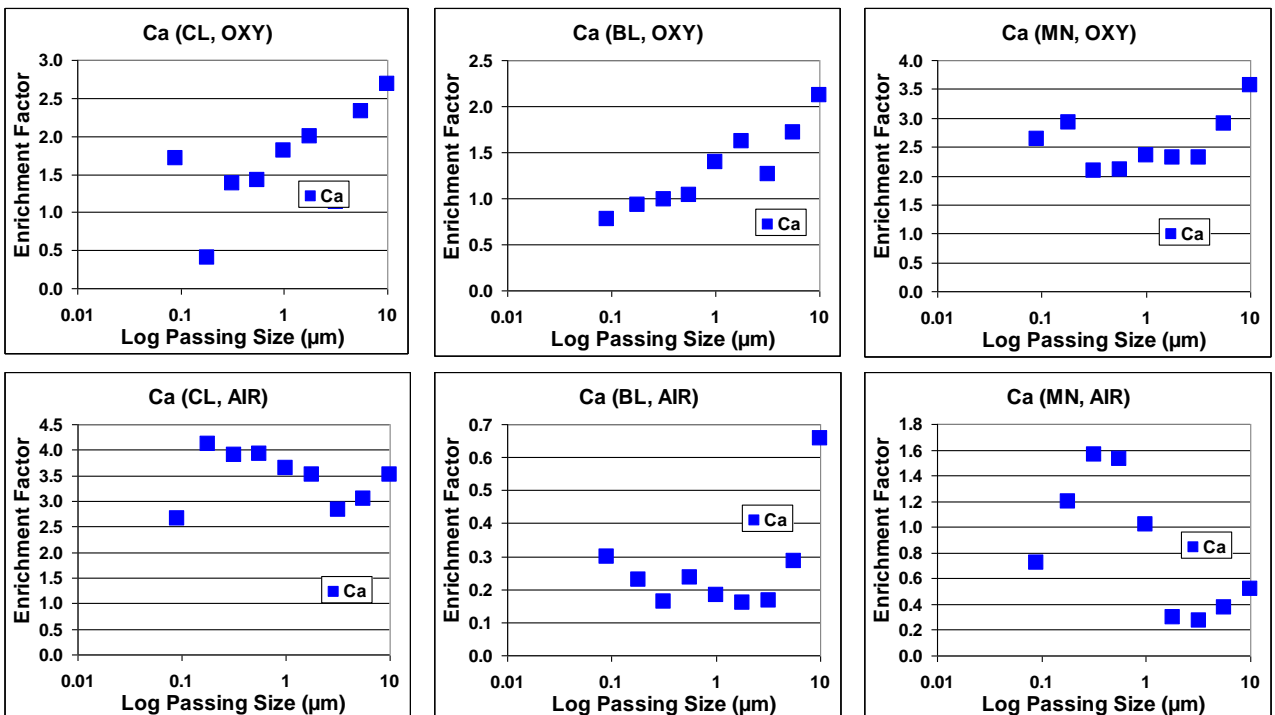


Figure 10 EF of titanium in coal ash as a function of size <10  $\mu\text{m}$

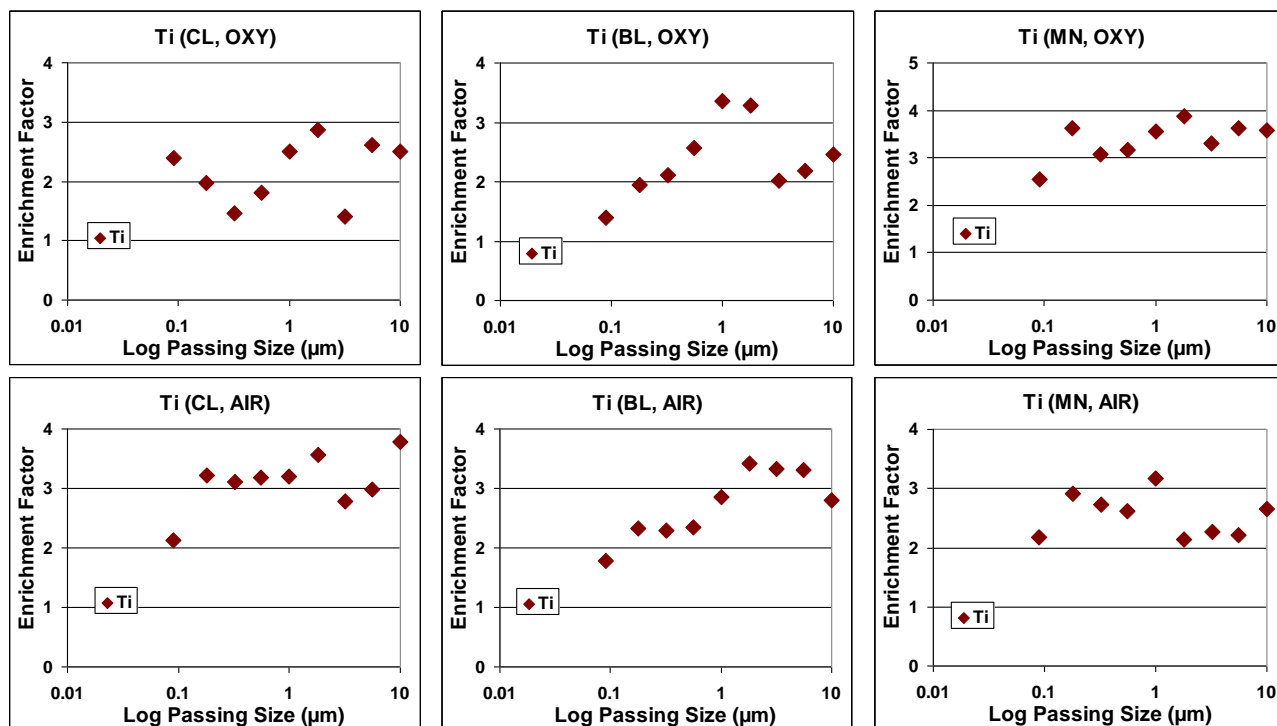


Figure 11 EF of iron in coal ash as a function of size <10  $\mu\text{m}$

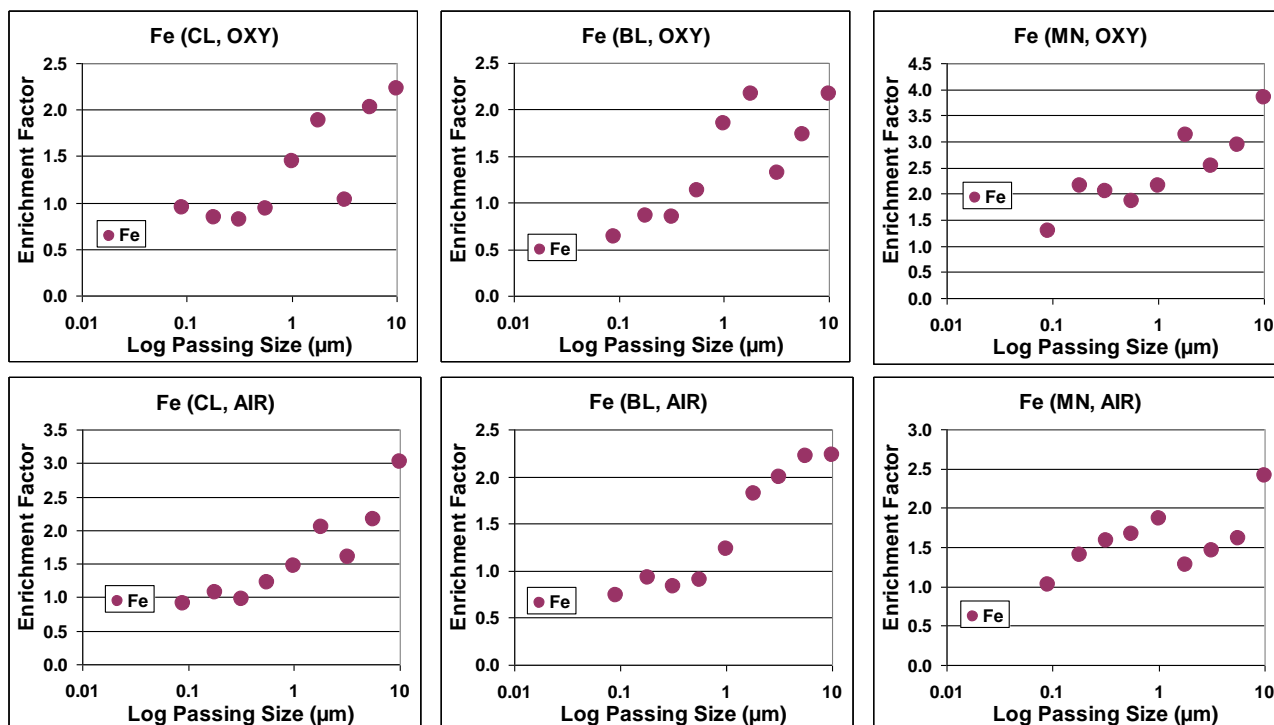
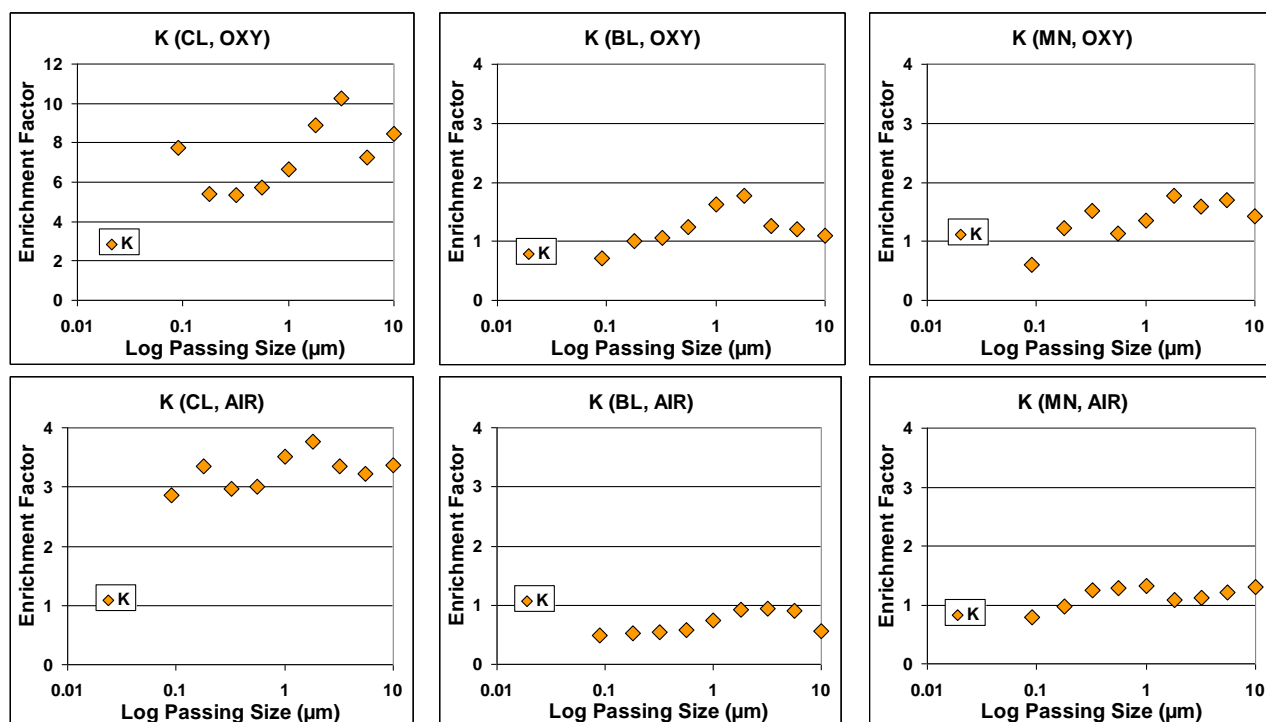


Figure 12 EF of potassium in coal ash as a function of size <10  $\mu\text{m}$



### 6.6.3 GROUP II(a) elements (Co, Cu, Ni)

Figure 13 EF of cobalt in coal ash as a function of size <10  $\mu\text{m}$ .

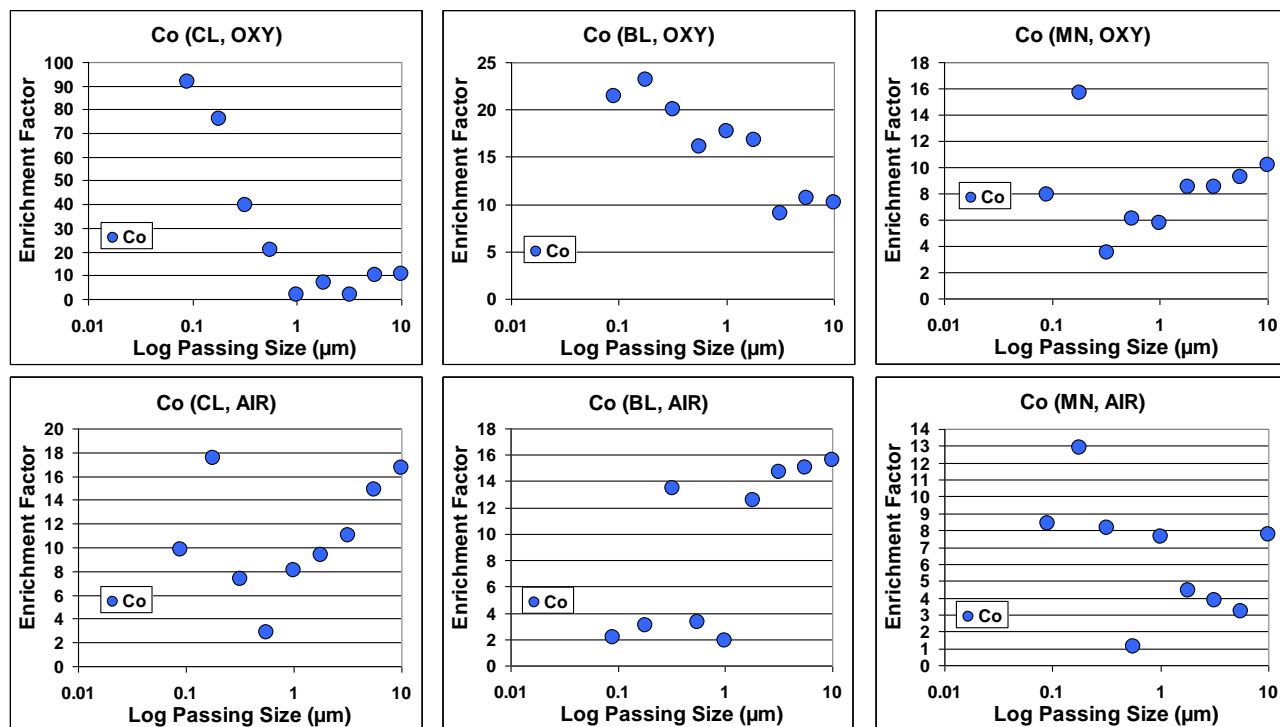


Figure 14 EF of copper in coal ash as a function of size <10  $\mu\text{m}$

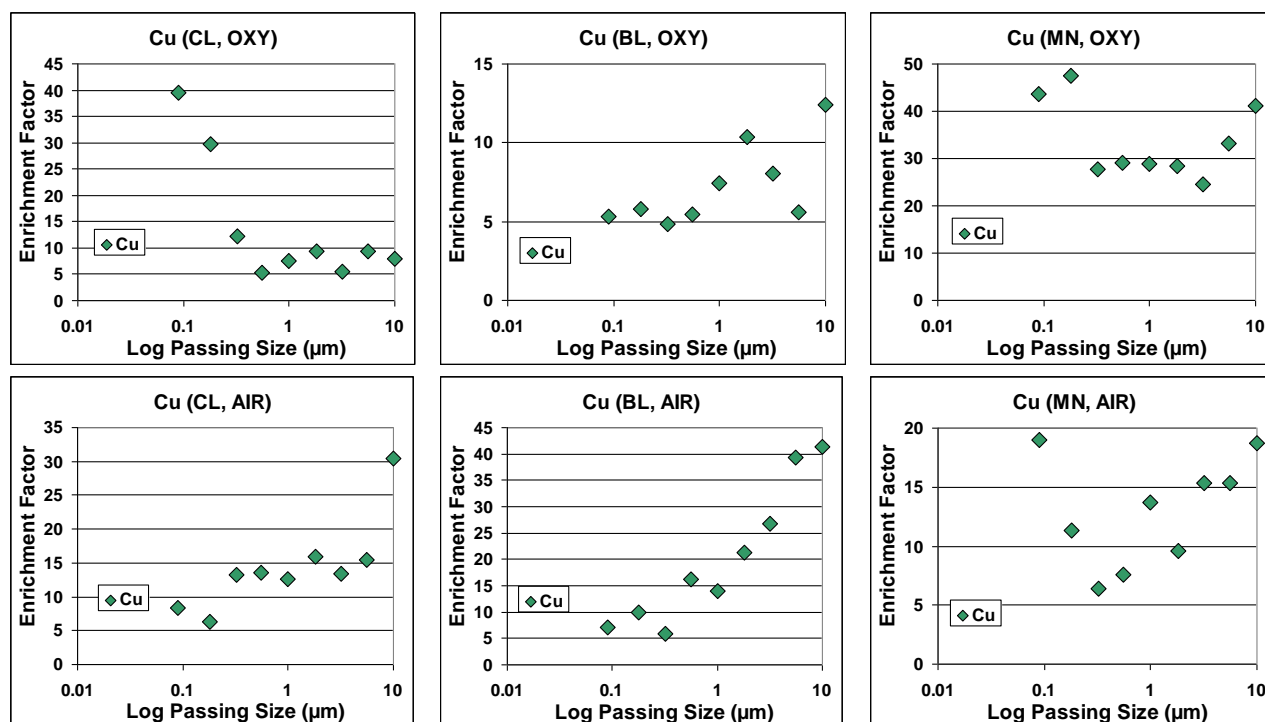
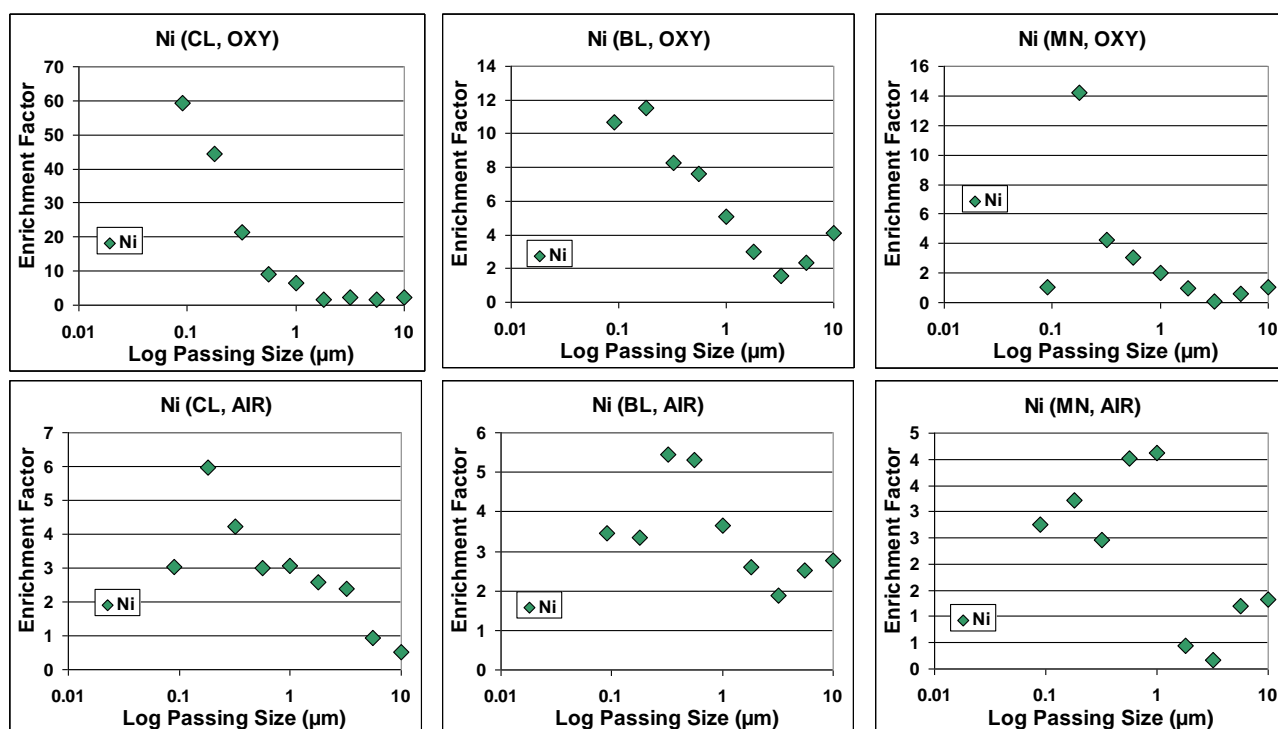


Figure 15 EF of nickel in coal ash as a function of size < 10  $\mu\text{m}$ .



## 6.6.4 GROUP II(b) elements (Cr, Mn)

Figure 16 EF of chromium in coal ash as a function of size <10  $\mu\text{m}$

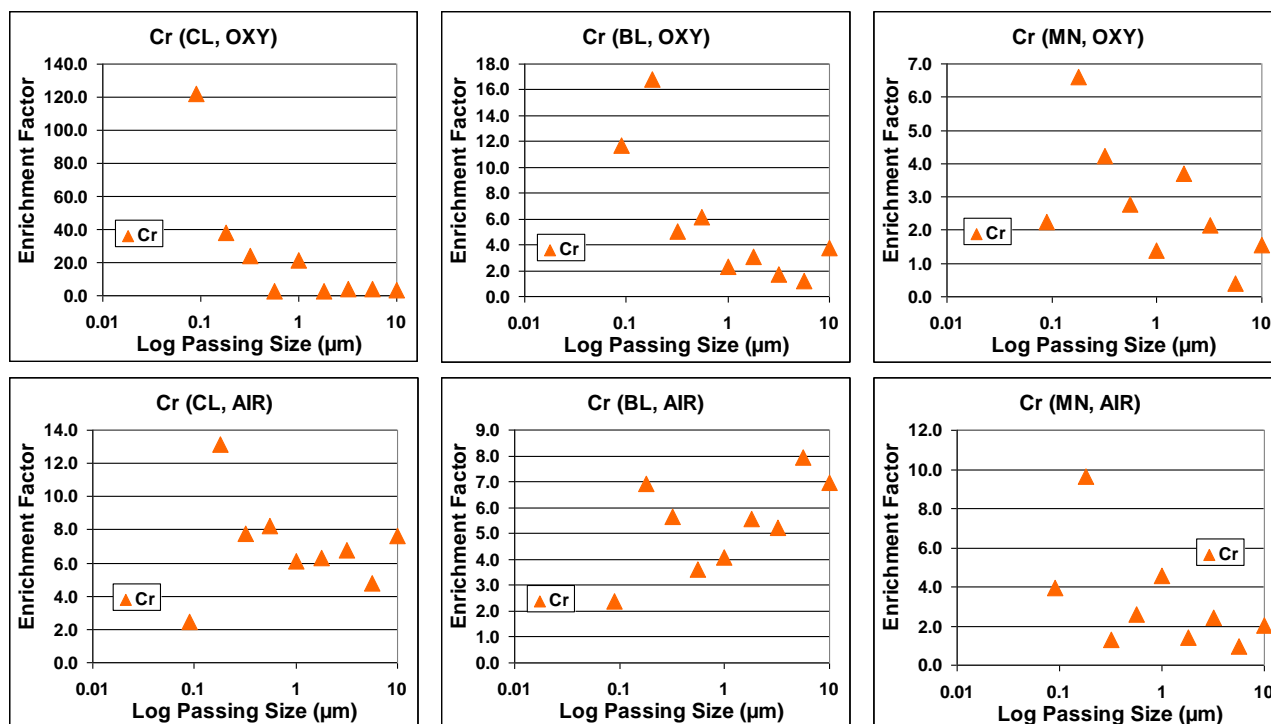
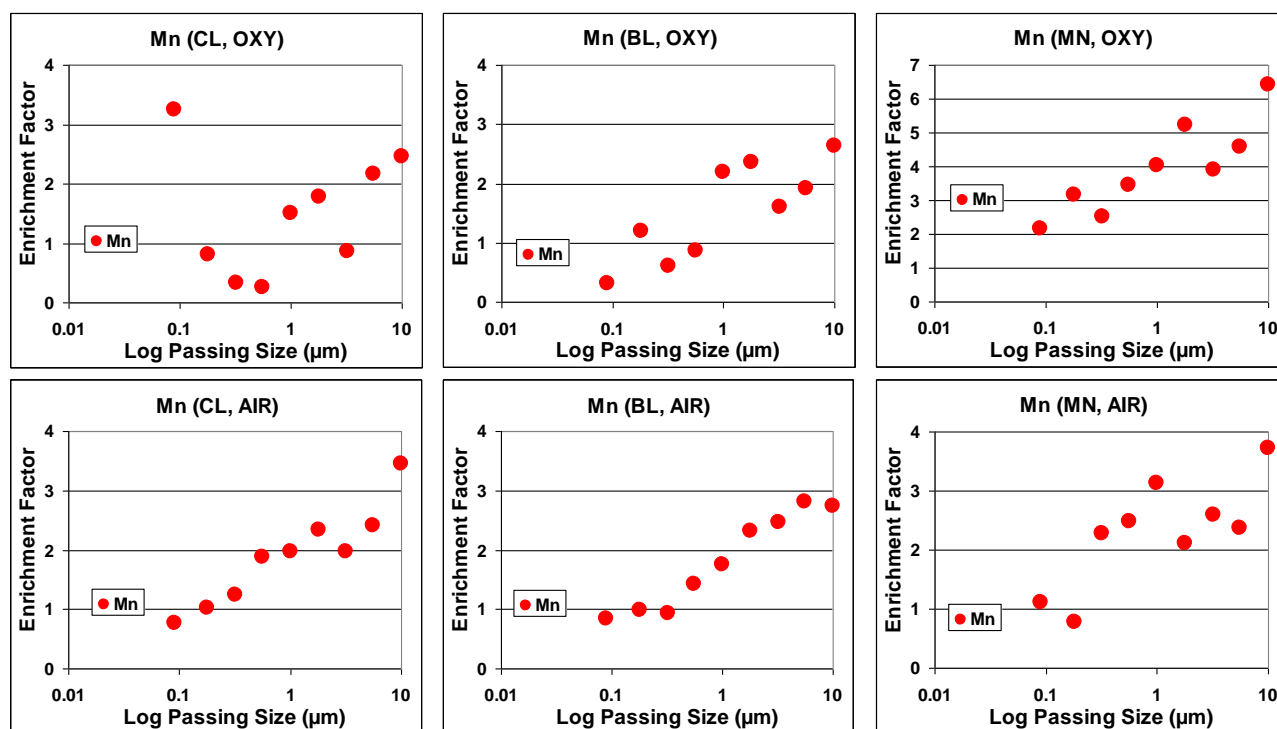


Figure 17 EF of manganese in coal ash as a function of size <10  $\mu\text{m}$



## 6.6.5 GROUP II(c) elements (Pb, Zn)

Figure 18 EF of lead in coal ash as a function of size <10  $\mu\text{m}$ .

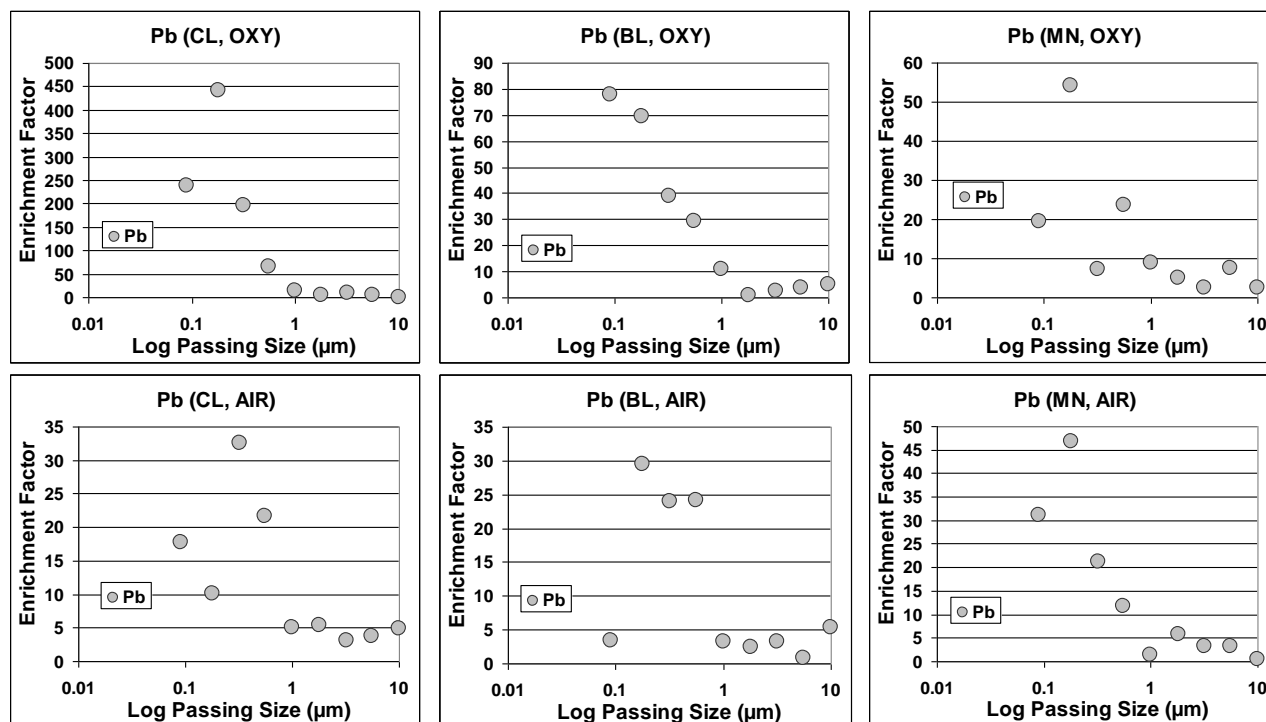
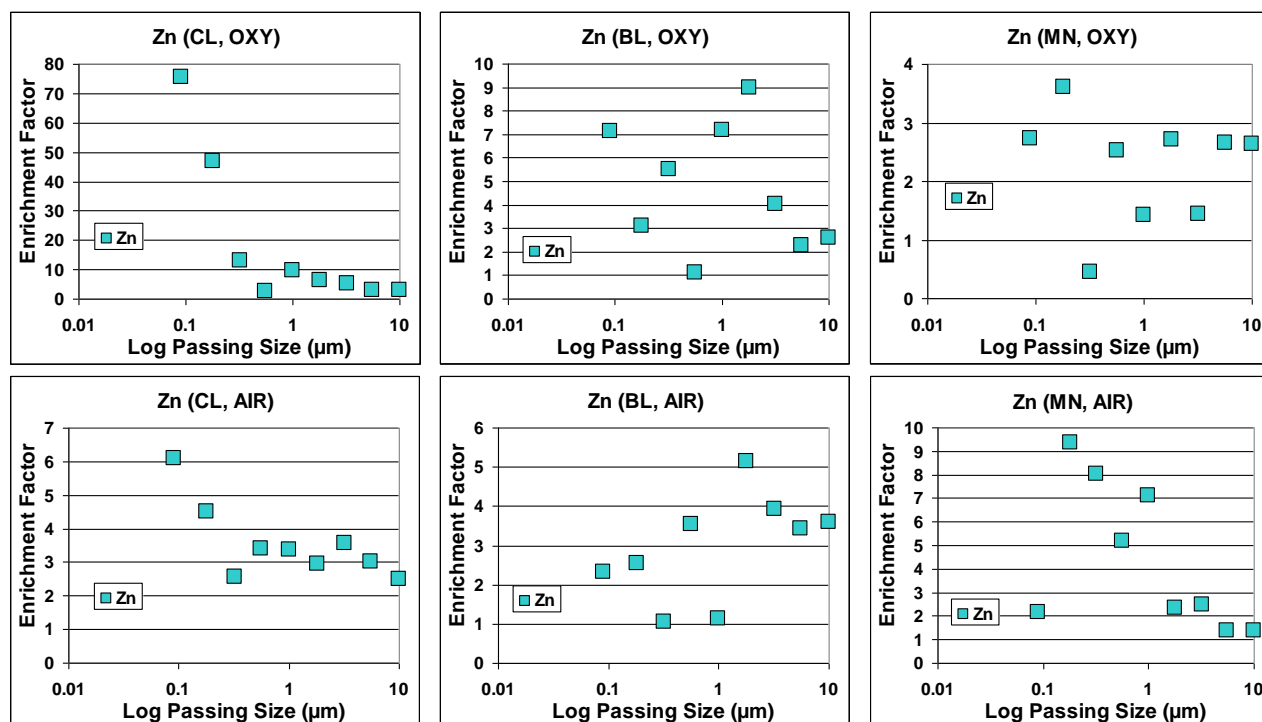


Figure 19 EF of zinc in coal ash as a function of size <10  $\mu\text{m}$ .



### 6.6.6 GROUP III elements (Br, Cl, S, Se)

Figure 20 EF of bromine in coal ash as a function of size <10  $\mu\text{m}$

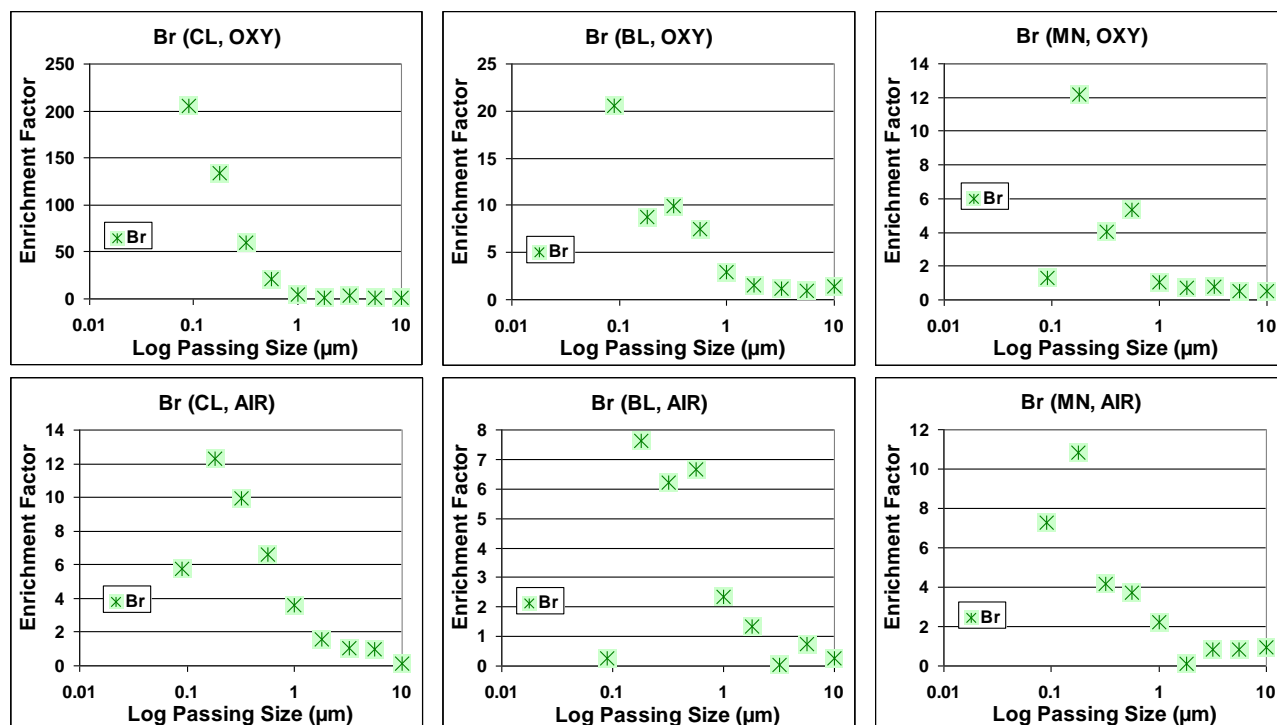


Figure 21 EF of chlorine in coal ash as a function of size <10  $\mu\text{m}$ .

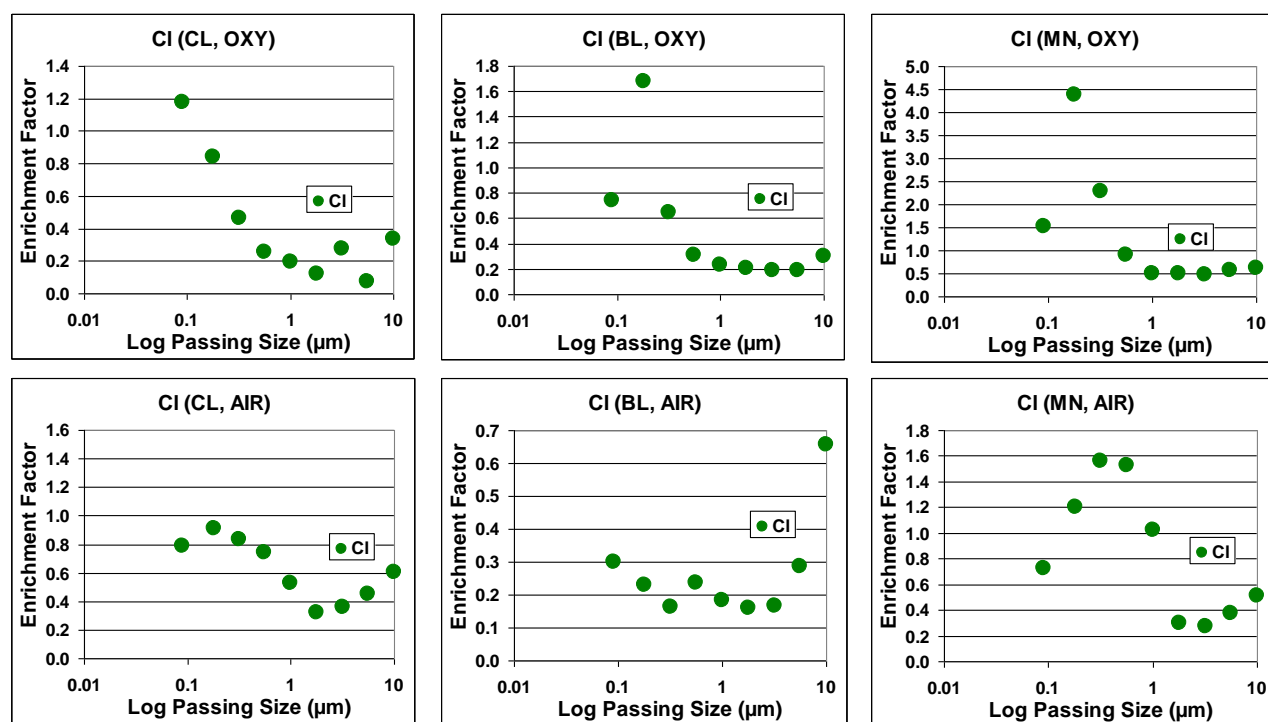




Figure 22 EF of sulfur in coal ash as a function of size <10  $\mu\text{m}$ .

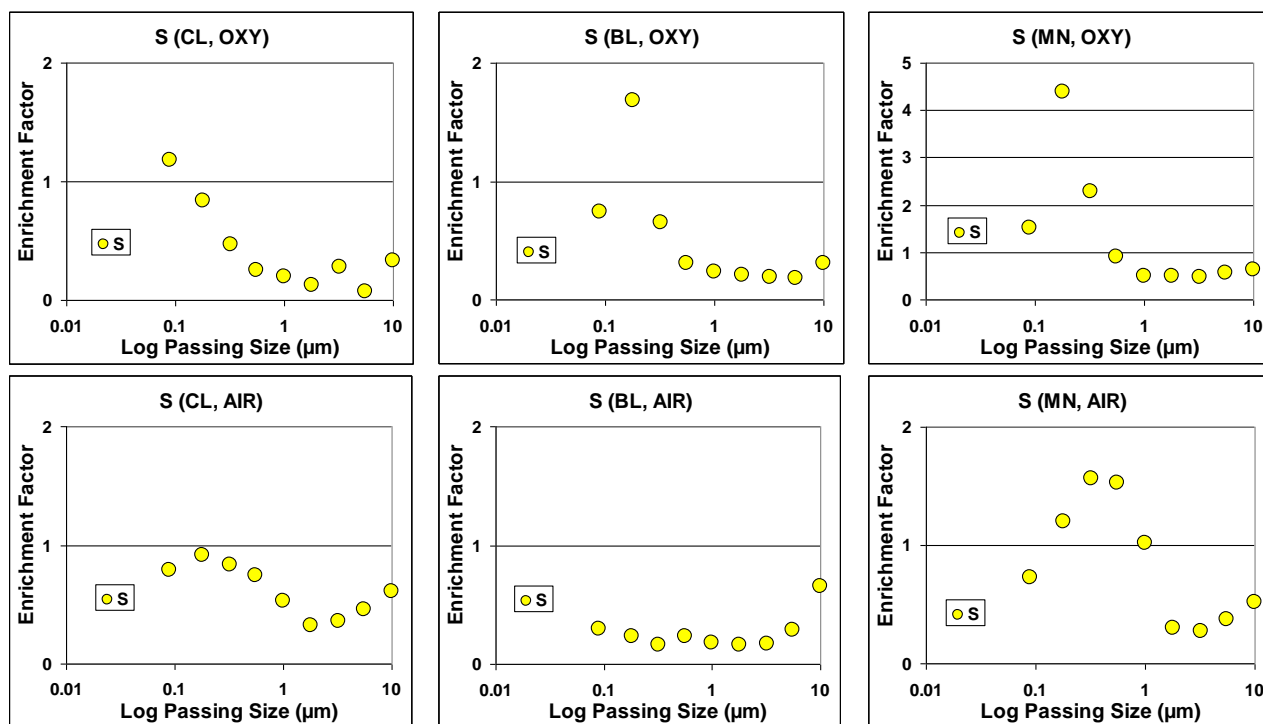
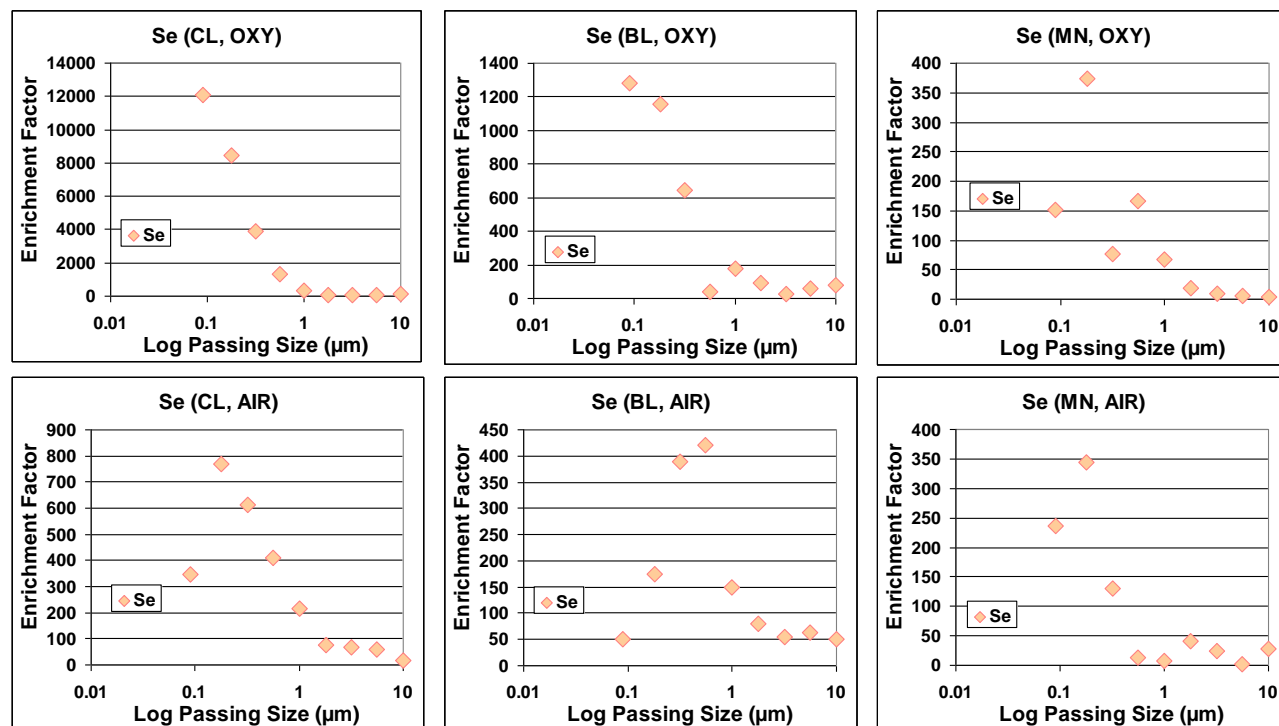


Figure 23 RF of selenium in coal ash as a function of size <10  $\mu\text{m}$ .



**Table 11 Summary of changes in EF with coal ash particle size and combustion conditions**

Meiji Group	Element	Enrichment behaviour over ash size range <0.18 – 10 µm	Variation between air and oxy-firing conditions from laboratory experiments
<b>GROUP I</b>			
	Si	Refractory, little variation over size range.	No apparent difference
	Ca	Apparent diminution in EF in smaller size fractions under oxy-firing, under air firing response more difficult to discern, possible indicating little change across size ranges under air-firing.	Lower EF in smaller size fraction under oxy-firing
	Ti	Refractory, small but inconsistent change over size range.	No apparent difference
	Fe	Consistent pattern of reduction in EF from the largest to smallest size fractions	No apparent difference
	K	No apparent change in EF across the size ranges under both air and oxy-firing	No apparent difference
<b>GROUP II</b>			
<b>I(a)</b>	Co	EF increases in smaller size fractions for the sub-bituminous coal (CL) and semi-anthracite/sub-bituminous blend (BL) under oxy-firing conditions. Under air firing EF is lower and appears to decrease with particle size. Bituminous coal (MN) shows the opposite trend.	Differences between oxy-firing and coal type.
	Cu	Under air-firing EF generally decreasing with decreasing particle size. Under oxy-firing indications that EF is stable except in the smallest size fraction where for BL and MN it increases.	Element seems more stable under oxy than air-firing
	Ni	EF generally increasing as particle size decreases, EF generally lower under air firing than oxy-firing.	Not significantly different, EF lower in air firing
<b>II(b)</b>	Cr	EF possibly increasing with decreasing particle size, generally higher under oxy-firing	Similar outcomes
	Mn	Consistent pattern of reduction in EF from the largest to smallest size fractions which parallels that for iron in Group I.	Similar outcomes
<b>II(c)</b>	Pb	Significant increase in EF in the particle size decreases under both oxy and air-firing, EF under oxy-firing conditions generally higher.	Similar outcome, EF generally higher under oxy conditions
	Zn	For coal CL EF increases with decreased at smallest size fractions, no consistency in coal BL results or coal MN under oxy firing condition. For coal MN EF steadily increases with decreasing particle size until the last size fraction when a reversion occurs.	Unclear

**Table 11** continued:

Meiji Group	Element	Enrichment behaviour over ash size range <0.18 – 10 µm	Variation between air and oxy-firing conditions from laboratory experiments
<b>GROUP III</b>			
	Br	Br scoured from larger particles (EF<1) and then EF increases rapidly as particle size decreases (below 1 µm) for all coals and firing conditions. For the smallest particle cut ((0-0.18 µm) there is then a significant decrease in EF.	Similar outcomes, higher EF under oxy conditions.
	Cl	For oxy-firing results are very similar to those for Br, under air-firing conditions low EFs indicate scouring of Cl from system. In the bituminous coal (MN) the reversion at the lowest particle size seen for Br is apparent.	Similar outcomes, different behaviours between coal types is apparent.
	S	S has been scoured from the particles and little redeposition has occurred. Some increase in EF apparent in the smaller size fractions and a reversion in EF in the smallest, with this most pronounced in the bituminous coal (MN)	Similar outcomes, different behaviours between coal types is apparent.
	Se	Extraordinary increases in EF for particles generally below 1 µm. Some reversion of EF at the smallest cut which is more apparent under air-fired conditions.	Similar behaviour, EF under oxy conditions significantly higher.

## **6.7 Relevance of EF results to the Callide Oxy-fuel process**

The results presented tend to show that for most elements that combustion under oxy-fuel like conditions (of high CO<sub>2</sub> and a lack of N<sub>2</sub>) makes little difference to the enrichment behaviour of the species examined, although it is possible that other differences in air and oxyfiring processing conditions (as used at Callide) may result in greater differences. A trend that EF in the smaller particles is higher under O<sub>2</sub>/CO<sub>2</sub> firing conditions becomes more pronounced as the volatility of the metallic elements increases (that is from Meiji's Group I through to Group III, see Table 10).

In Group III, the sole metallic element which could be examined was Se and the concentration changes in the smallest size fractions for this element were very high, as indicated by the rapid increases in EF. These changes may have implications for oxy-fuelled plant operation as these very fine particles are more likely to pass through the fabric filtration system and either be recirculated to the burners or alternatively to the CO<sub>2</sub> processing unit to be removed in the gas scrubbing systems.

This effect needs to be followed up for Hg, the other significant Group III metallic element, as it is unfortunate that PIXIE is unable to measure this element at the low levels encountered in the ash samples. For this to be possible further development of the MOUDI capture system will be required using alternative substrates and analytical systems. Also given the importance already demonstrated of carbon in ash to Hg capture a method for estimation of this component on the MOUDI substrates needs to be devised for this work to be more meaningful.

Earlier in this report it was noted that there seems to be some enrichment of Cr in the latter hoppers in the FF collection train and it was hypothesised that this may be due to increased fineness of the collected material. This conclusion seems to be supported by the results shown in Figure 16 where increases in EF for Cr are seen as particle size decreases.

A contrary result to this trend for Group II(b) is Mn, and this is interesting as it consistently goes against this trend with a pattern of more depletion (decreasing EF) in smaller sized particles and mirrors the behaviour of Fe in Group I (compare Figure 11 with Figure 17).

## 7. CONCLUSIONS

### 7.1 *Project extension*

- An examination of environmentally available chromium (determined by an aggressive acid digestion) in all ash and coal samples from the field trials has shown levels to be low (4.4 - 8.4 mg/kg). This is 10-15% of the total chromium, the remainder of which is isolated within the siliceous glass matrix of the ash and not available to leaching environmental fluids. These levels are significantly lower than health based investigation levels for soils containing Cr of 100 mg/kg.
- The carcinogenic hexavalent form of chromium [Cr(VI)] was below the normal limit of reporting of 0.5 mg/kg. Re-evaluation of these data using a lower detection limit of 0.05 mg/kg (with inherent high errors in quantification) showed that this species was likely present at very low levels in some of the fly ash samples.
- There seems to be a potential relationship between, increased levels of chromium, the detection of low levels of Cr(VI)] and finer sized fly ash particles. A relationship which has been given further credence by laboratory measurements showing increased enrichment factors for chromium as ash particle decreases.
- The quality of the produced CO<sub>2</sub> from the Callide CPU for a wide range of elements has been assessed for potential use in the food industry, a more stringent standard than that required for pipeline quality for use in enhanced oil recovery or CCS.
- For the elements measured during the field trial all concentration values in the CO<sub>2</sub> produced by the CPU were orders of magnitude lower than the levels which might be required for use in the beverage industry, the MDL for sulfur is close to the limits of 0.6 mg/Nm<sup>3</sup>. CO<sub>2</sub> specifications include a number of compounds, particularly hydrocarbons and water, which require further testing to ensure compliance.
- Quantitative modelling of mercury emissions from the Callide plant was carried out using the iPOG software package developed in conjunction with the United Nations Environment Program (UNEP) Mercury Partnerships. Input data for the model were the plant conditions measured during the field trial and the model estimates were compared to measurements of mercury capture made during the field trials.
- It was shown that if carbon in ash exceeds ~5% more than 90% of the mercury is captured in the fabric filters. For lower levels of carbon in ash mercury capture reduces to 60-80%. iPOG calculations reproduce these results with reasonable precision for air-fired conditions. Agreement for oxy-fired conditions is poorer which may be due to the source of the data used to develop iPOG.
- The modelling and direct measurement suggest that substantial amounts of contained mercury can be removed from the gas stream by the carbon present in the ash. As a result for some operating conditions at Callide most of the mercury will not be transported to the CPU but will require management through the ash stream.

- The strong relationship between mercury capture and carbon in ash suggests that in new build plants with higher combustion efficiencies and consequent lower carbon in ash, an increased proportion of available mercury will be transported to the CPU.
- A laboratory examination of elemental enrichment behaviour in fine particles (<10 µm) was carried out using Meiji's model of elemental behaviour in combustion systems.
- The results showed that for most elements combustion under one difference between air and oxy-fuel like conditions (of high CO<sub>2</sub> and a lack of N<sub>2</sub>) makes little difference to the pattern of enrichment behaviour of the species.
- For the sixteen elements examined, a trend was generally apparent that the more volatile elements (Group III in Meiji's model) are enriched in in the smaller particles under oxy-firing conditions. The other elements show little change in Enrichment Factor as a function of either fly ash particle size or air verses oxy-firing conditions.
- Selenium (a volatile Group II metallic element) showed rapid increases in EF in the smallest size fractions and effect which may have implications for oxy-fuelled plant operation. These very fine particles (containing high Se levels) are more likely to pass through the fabric filtration system and either be recirculated to the burners or alternatively to the CO<sub>2</sub> processing unit to be removed in the gas scrubbing systems.

## **7.2 Project Overall**

- The project was successful in meeting its scope and objectives.
- The health and environmental outcomes under oxy-firing conditions are likely to be similar to those achieved when using conventional air-firing.
- Levels of metals, acid gases and mercury in particular, are below the level of operational concern in the CPU beyond the first low pressure scrubber.
- The results show that the trace element content of the feed coals used in the program are very similar for most elements determined with the exception of Ba, B and Mn.
- Mercury contents in the produced ash varied widely, with most deposited in the flyash fraction where concentrations ranged from 43 – 270 ng/g.
- Modelling and measurement of mercury behaviour in the combustion system showed the strong relationship between carbon in ash and mercury partitioning into the ash fraction. This may have implications which should be examined for plants which operate at higher efficiency and consequent lower carbon in ash.
- Approximately 80% of mercury in CPU process gas was removed by the initial low pressure scrubber; with the final CPU process gas mercury concentration approaching the concentrations measured in ambient air (<2 ng/m<sup>3</sup>).
- Halogens (Br, Cl and F) were at or below detection limits for the sampling techniques in both the stack and CPU. Halides (HBr, HCl and HF) were detectable in the stack

(but not in the CPU), although no consistent trend in the field trial results between coal type or firing mode (oxy or air fired) was apparent. Laboratory work suggests that depletion of these species from the coal and ash occurs in all but the finest of particle sizes.

- Overall trace metal concentrations detected in both the gas and solids phases are low and should have minimal environmental impact.
- From the field trials some differences in partitioning to the gas phase were apparent with three groups of elements identified:
  - low level partitioning (<5%) for most metals studied (As, Be, Co, Cu, Pb, Mn);
  - a group where retention in the gas phase is consistently higher; Sb (5.5 – 8.8%), B (16.2 – 40.4%), Cd (9.1 – 40.7%) and Se (8.1 – 55%);
  - for three elements Cr, Ni and Zn there is a lack of consistency in the outcomes which may have resulted from analytical imprecision and/or sampling errors.
- From the field trial results it did not appear that partitioning of trace metals to the gas phase at the stack is a function of either firing condition (oxy or air-firing) or coal type. Follow up laboratory studies have shown potential mechanisms via particle elemental enrichment for this behaviour, although a trend in higher volatility elements to greater enrichment in the smallest particles during oxy-firing is also apparent.
- These results for metal partitioning following combustion are generally consistent with the behaviour found by other researchers.
- Concentrations of metals measured in the CPU process gas beyond the first lower pressure scrubber were at or around MDL values. At these metal concentrations the produced CO<sub>2</sub> would comply with the specifications for the food and beverage industry. Although the presence or concentration of other compounds which were not tested which may preclude this use.
- Under air-firing conditions SO<sub>2</sub> concentrations in the stack gases were three to four times lower than during oxy-firing. Laboratory studies confirmed the almost complete depletion of sulfur from the ash samples, so the probable influence of feed coal sulfur on concentrations observed in the field trials is unsurprising.
- In the CPU levels of SO<sub>x</sub> were at or below the MDLs, for both SO<sub>2</sub> and for SO<sub>3</sub>. The results demonstrate that the sulfur in the process gas stream has been removed effectively from the CPU process gas by the initial low pressure scrubber.

## 8. REFERENCES

- Bool, L. E. and J. J. Helble (1995). "A laboratory study of the partitioning of trace elements during pulverized coal combustion." Energy & Fuels **9**(5): 880-887.
- Chen, J., F. Jiao, L. Zhang, H. Yao and Y. Ninomiya (2012). "Use of Synchrotron XANES and Cr-Doped Coal to Further Confirm the Vaporization of Organically Bound Cr and the Formation of Chromium(VI) During Coal Oxy-Fuel Combustion." Environmental Science & Technology **46**(6): 3567-3573.
- Cohen, D. D., G. M. Bailey and R. Kondepudi (1996). "Elemental analysis by PIXE and other IBA techniques and their application to source fingerprinting of atmospheric fine particle pollution." Nuclear Instruments & Methods in Physics Research Section B-Beam Interactions with Materials and Atoms **109**: 218-226.
- Cohen, D. D., E. Stelcer, O. Hawas and D. Garton (2004). "IBA methods for characterisation of fine particulate atmospheric pollution: a local, regional and global research problem." Nuclear Instruments & Methods in Physics Research Section B-Beam Interactions with Materials and Atoms **219-20**: 145-152.
- Darakas, E., V. Tsiridis, M. Petala and A. Kungolos (2013). "Hexavalent chromium release from lignite fly ash and related ecotoxic effects." Journal of Environmental Science and Health Part a-Toxic/Hazardous Substances & Environmental Engineering **48**(11): 1390-1398.
- Davis, C. M. and J. B. Vincent (1997). "Chromium in carbohydrate and lipid metabolism." Journal of Biological Inorganic Chemistry **2**(6): 675-679.
- Dhal, B., H. N. Thatoi, N. N. Das and B. D. Pandey (2013). "Chemical and microbial remediation of hexavalent chromium from contaminated soil and mining/metallurgical solid waste: A review." Journal of Hazardous Materials **250**: 272-291.
- EIGA (2008). Carbon dioxide source qualification quality standards and verification: IGC Doc 70/08/E. Brussels, European Industrial Gases Association AISBL.
- enHealth (2001). Health based soil investigation levels, Commonwealth of Australia, Department of Health.
- Finkelman, R. B. (1999). "Trace elements in coal - Environmental and health significance." Biological Trace Element Research **67**(3): 197-204.
- Furtmann, K. and D. Seifert (1990). "On the routine determination of chromium (VI) in soils." Fresenius' Journal of Analytical Chemistry **338**(1): 73-74.
- Goodarzi, F. and F. E. Huggins (2005). "Speciation of chromium in feed coals and ash byproducts from Canadian power plants burning subbituminous and bituminous coals." Energy & Fuels **19**(6): 2500-2508.
- Haynes, B. S., M. Neville, R. J. Quann and A. F. Sarofim (1982). "Factors governing the surface enrichment of fly ash in volatile trace species." Journal of Colloid and Interface Science **87**(1): 266-278.
- Helble, J. J. (1994). "Trace element behavior during coal combustion: results of a laboratory study." Fuel Processing Technology **39**(1-3): 159-172.
- Huang, Y. J., B. S. Jin, Z. P. Zhong, X. Rui, Z. Y. Tang and H. F. Ren (2004). "Occurrence and volatility of several trace elements in pulverized coal boiler." Journal of Environmental Sciences-China **16**(2): 242-246.
- Huggins, F. E., G. P. Huffman and J. D. Robertson (2000). "Speciation of elements in NIST particulate matter SRMs 1648 and 1650." Journal of Hazardous Materials **74**(1-2): 1-23.
- Jia, Y. and J. S. Lighty (2012). "Ash particulate formation from pulverized coal under Oxy-Fuel combustion conditions." Environmental Science & Technology **46**: 5214-5221.



- Kazanc, F., Y. A. Levendis and T. Maffei (2013). "Chemical Composition of Submicrometer Particulate Matter (PM<sub>1</sub>) Emitted from Combustion of Coals of Various Ranks in O<sub>2</sub>/N<sub>2</sub> and O<sub>2</sub>/CO<sub>2</sub> Environments." Energy & Fuels **27**(8): 4984-4998.
- Kimbrough, D. E., Y. Cohen, A. M. Winer, L. Creelman and C. Mabuni (1999). "A Critical Assessment of Chromium in the Environment." Critical Reviews in Environmental Science and Technology **29**(1): 1-46.
- Kingston, H. M., R. Cain, D. W. Huo and G. M. M. Rahman (2005). "Determination and evaluation of hexavalent chromium in power plant coal combustion by-products and cost-effective environmental remediation solutions using acid mine drainage." Journal of Environmental Monitoring **7**(9): 899-905.
- Maffei, T., R. Khatami, S. Pierucci, T. Faravelli, E. Ranzi and Y. A. Levendis (2013). "Experimental and modeling study of single coal particle combustion in O<sub>2</sub>/N<sub>2</sub> and Oxy-fuel (O<sub>2</sub>/CO<sub>2</sub>) atmospheres." Combustion and Flame **160**(11): 2559-2572.
- Malherbe, J., M.-P. Isaure, F. SÃ©by, R. P. Watson, P. Rodriguez-Gonzalez, P. E. Stutzman, C. W. Davis, C. Maurizio, N. Unceta, J. R. Sieber, S. E. Long and O. F. X. Donard (2011). "Evaluation of Hexavalent Chromium Extraction Method EPA Method 3060A for Soils Using XANES Spectroscopy." Environmental Science & Technology **45**(24): 10492-10500.
- Marple, V. A., K. L. Rubow and S. M. Behm (1991). "A Microorifice Uniform Deposit Impactor (MOUDI): Description, Calibration, and Use." Aerosol Science and Technology **14**(4): 434 - 446.
- Meij, R. (1994). "Trace-element behavior in coal-fired power plants." Fuel Processing Technology **39**(1-3): 199-217.
- Meij, R. and H. t. Winkel (2007). "The emissions of heavy metals and persistent organic pollutants from modern coal-fired power stations." Atmospheric Environment **41**(40): 9262-9272.
- Morrison, A. L., P. F. Nelson, P. S. Bray and H. Malfroy (2014). Impacts of trace components on Oxy-combustion for the Callide Oxy-fuel Project-Results from Callide fieldtrials, December 2012, Macquarie University, Graduate School of the Environment.
- Nelson, P. F. (2013). Impacts of trace components on Oxy-combustion for the Callide Oxy-fuel Project - Literature Review, Graduate School of the Environment, Macquarie University, North Ryde, NSW.
- NHMRC (2004). National Water Quality Management Strategy: Australian Drinking Water Guidelines. Canberra, ACT, Australian Government.
- Nriagu, J. O. and E. Nieboer, Eds. (1988). Chromium in the Natural and Human Environments. New York, USA, Wiley.
- Querol, X., J. L. FernÃ¡ndez-Turiel and A. LÃ³pez-Soler (1995). "Trace elements in coal and their behaviour during combustion in a large power station." Fuel **74**(3): 331-343.
- Rabinowitz, M. B., H. C. Gonick, S. R. Levin and M. B. Davidson (1983). "EFFECTS OF CHROMIUM AND YEAST SUPPLEMENTS ON CARBOHYDRATE AND LIPID-METABOLISM IN DIABETIC MEN." Diabetes Care **6**(4): 319-327.
- Shaffer, R. E., J. O. Cross, S. L. Rose-Pehrsson and W. T. Elam (2001). "Speciation of chromium in simulated soil samples using X-ray absorption spectroscopy and multivariate calibration." Analytica Chimica Acta **442**(2): 295-304.
- Shanker, A. K., C. Cervantes, H. Loza-Tavera and S. Avudainayagam (2005). "Chromium toxicity in plants." Environment International **31**(5): 739-753.
- Song, W., F. Jiao, N. Yamada, Y. Ninomiya and Z. Zhu (2013). "Condensation Behavior of Heavy Metals during Oxy-fuel Combustion: Deposition, Species Distribution, and Their Particle Characteristics." Energy & Fuels **27**(10): 5640-5652.

- Sporl, R., L. Belo, K. Shah, R. Stanger, R. Giniyatullin, J. Maier, T. Wall and G. Scheffknecht (2014). "Mercury Emissions and Removal by Ash in Coal-Fired Oxy-fuel Combustion." Energy & Fuels **28**(1): 123-135.
- Stam, A. F., R. Meij, H. te Winkel, R. J. v. Eijk, F. E. Huggins and G. Brem (2011). "Chromium Speciation in Coal and Biomass Co-Combustion Products." Environmental Science & Technology **45**(6): 2450-2456.
- Stelcer, E., A. L. Morrison, A. Atanacio and D. D. Cohen (2011). PIXE analysis of MOUDI filters. Clean Air Society of Australia and New Zealand (CASANZ) Auckland, NZ.
- Swaine, D. J. and F. Goodarzi (1995). Environmental aspects of trace elements in coal. Dordrecht, The Netherlands, Kluwer.
- Toftegaard, M. B., J. Brix, P. A. Jensen, P. Glarborg and A. D. Jensen (2010). "Oxy-fuel combustion of solid fuels." Progress In Energy And Combustion Science **36**(5): 581-625.
- UNIDO (2011). Global technology roadmap for CCS in industry. Sectoral assessment: CO2 enhanced oil recovery. Geneva, United Nations Industrial Development Organization.
- USEPA (1994a). Method 200.2 Sample preparation procedure for the spectrochemical determination of total recoverable elements. USEPA. Washington, DC.
- USEPA (1994b). Method 200.8 Determination of Trace Elements in Waters and Wastes by Inductively Coupled Plasma - Mass Spectrometry. U. S. EPA. Washington, DC.
- USEPA (1996a). Method 3060A, alkaline digestion for hexavalent chromium. U. S. EPA. Washington, DC.
- USEPA (1996b). Methods 3050A and 3050B Acid Digestion of Sediments, Sludges and Soil. USEPA. Washington, DC.
- USEPA (2007). Method 6020 Determination of trace metals by ICP-MS. USEPA. Washington, DC.
- Vincent, J. B. (2004). "Recent developments in the biochemistry of chromium(III)." Biological Trace Element Research **99**(1-3): 1-16.
- Wall, T., R. Stanger and Y. Liu (2013). "Gas cleaning challenges for coal-fired oxy-fuel technology with carbon capture and storage." Fuel **108**: 85-90.
- Wang, C. A., Y. B. Du and D. F. Che (2012). "Investigation on the NO Reduction with Coal Char and High Concentration CO during Oxy-fuel Combustion." Energy & Fuels **26**(12): 7367-7377.
- WHO (2008). Guidelines for Drinking-water Quality (THIRD EDITION). Geneva, World Health Organization.
- Xu, M. H., R. Yan, C. G. Zheng, Y. Qiao, J. Han and C. D. Sheng (2003). "Status of trace element emission in a coal combustion process: a review." Fuel Processing Technology **85**(2-3): 215-237.
- Zhao, Y. C., J. Y. Zhang and C. G. Zheng (2013). "Release and removal using sorbents of chromium from a high-Cr lignite in Shenbei coalfield, China." Fuel **109**: 86-93.

## Appendix A Photographs of collected substrates showing coal ash distribution

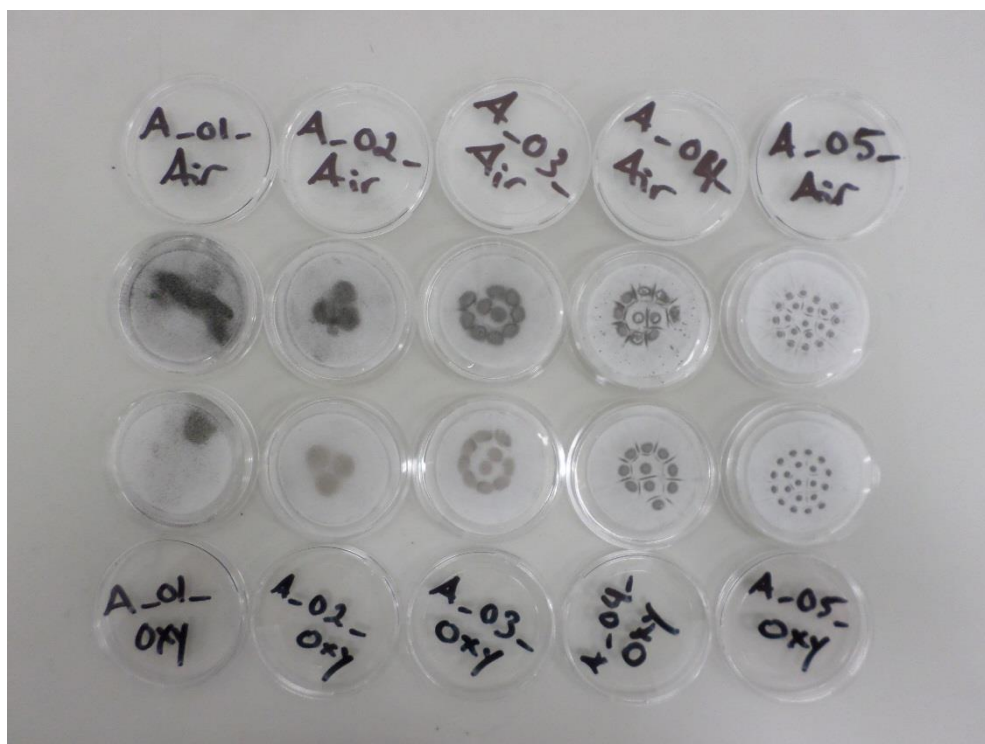


Figure A1 . Top row from left to right: CL coal ash stages 1-5 Air fired. Bottom row from left to right: CL coal ash stages 1-5 Oxy fired.

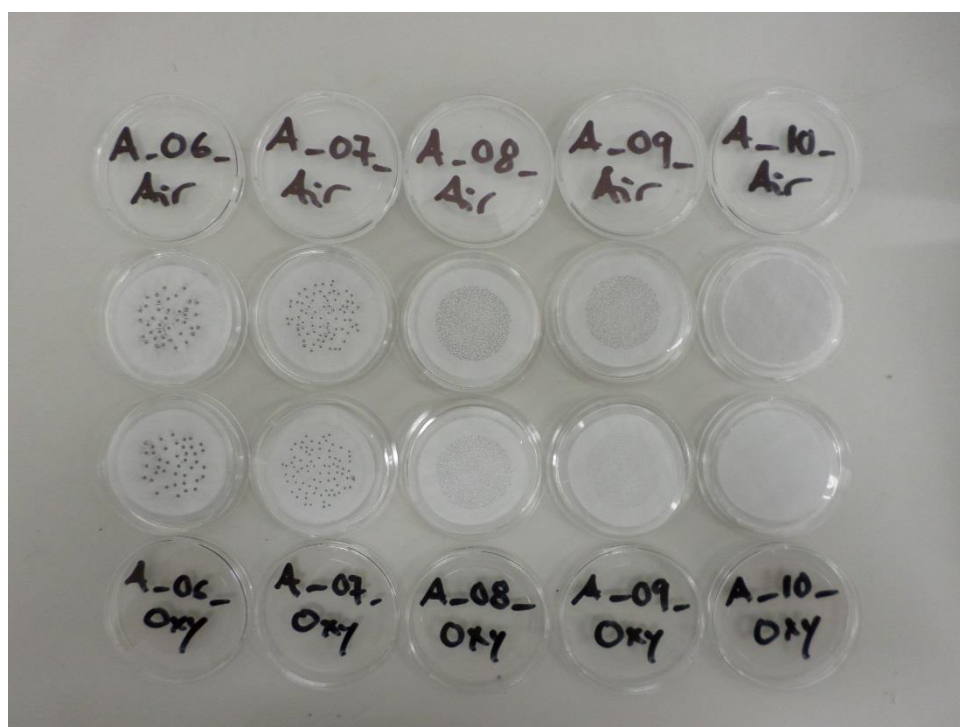


Figure A2. Top row from left to right: CL coal ash stages 6-10 Air fired. Bottom row from left to right: CL coal ash stages 6-10 Oxy fired.

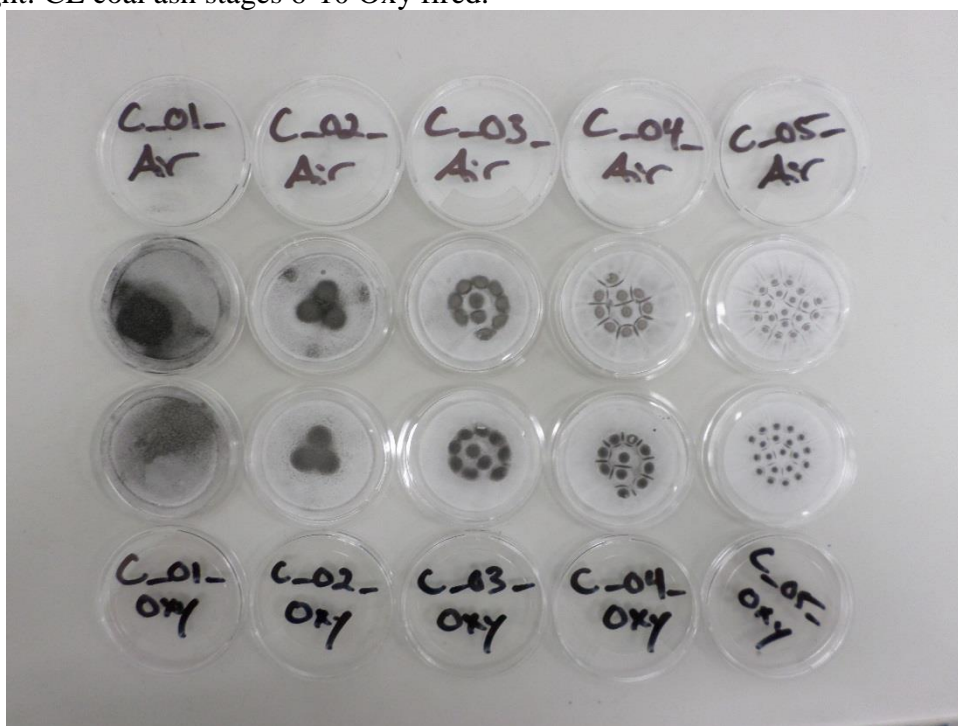


Figure A3. Top row from left to right: BL coal ash stages 1-5 Air fired. Bottom row from left to right: BL coal ash stages 1-5 Oxy fired.

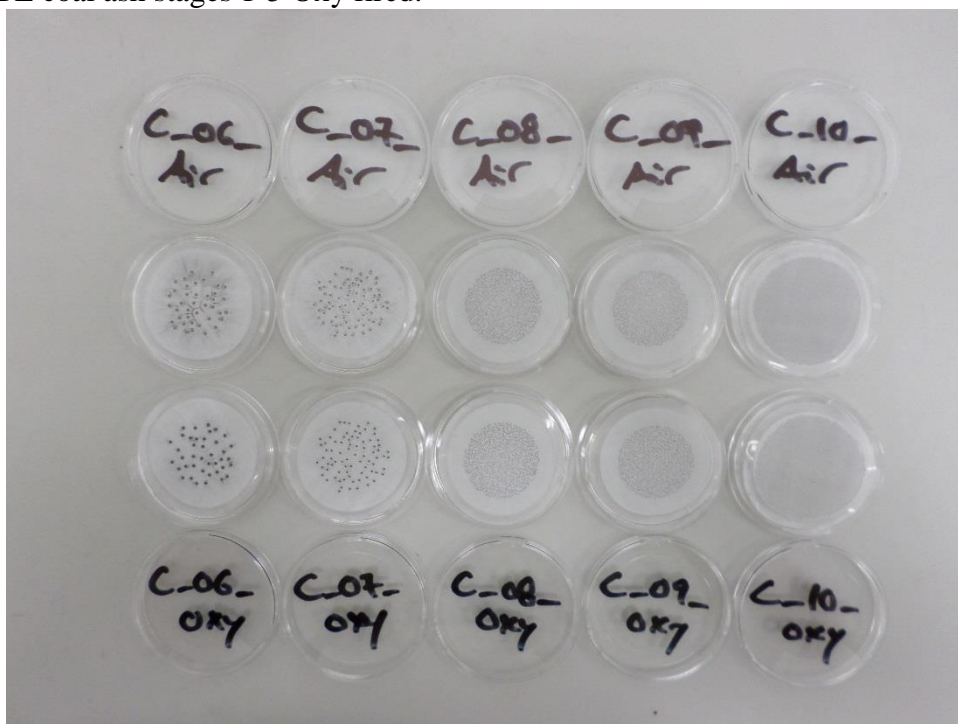


Figure A4. Top row from left to right: BL coal ash stages 6-10 Air fired. Bottom row from left to right: BL coal ash stages 6-10 Oxy fired.



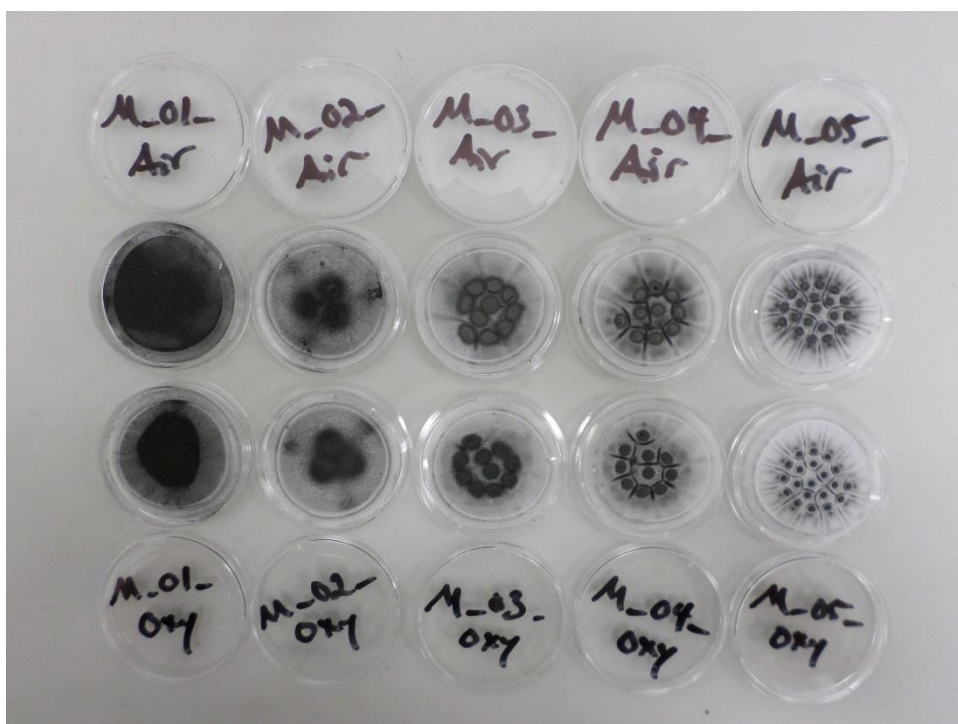


Figure A5. Top row from left to right: ML coal ash stages 1-5 Air fired. Bottom row from left to right: ML coal ash stages 1-5 Oxy fired.

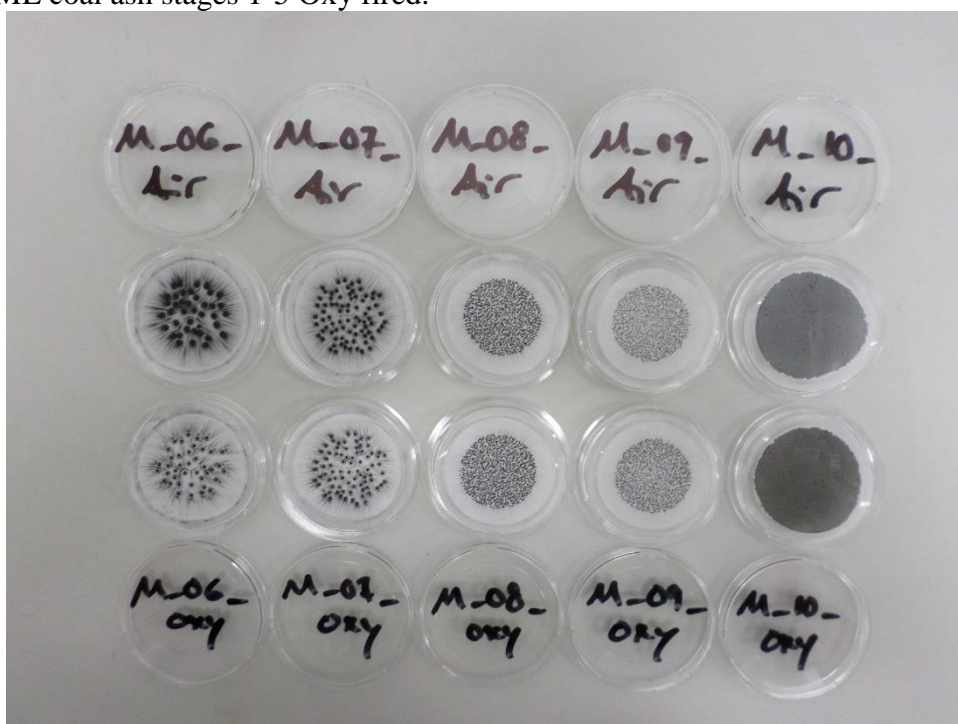


Figure A6. Top row from left to right: ML coal ash stages 6-10 Air fired. Bottom row from left to right: ML coal ash stages 6-10 Oxy fired.

## Appendix B IBA analysis of ash samples from drop tube experiments

### IBA results, coal CL Air Fired

MOUDI STAGE	F(197) ug/cm2	Na(440) ug/cm2	AL ug/cm2	SI ug/cm2	P ug/cm2	S ug/cm2	CL ug/cm2	K ug/cm2	CA ug/cm2	TI ug/cm2	V ug/cm2
1	0.645	1.056	7.214	10.860	0.018	0.856	0.047	0.140	0.858	1.092	0.008
2	0.611	1.178	73.167	105.401	0.050	1.755	0.096	1.890	7.996	14.064	0.129
3	0.651	0.477	37.709	53.548	0.036	0.675	0.030	0.932	3.564	5.707	0.027
4	256.268	0.000	34.110	46.762	0.034	0.483	0.013	0.875	3.003	4.806	0.010
5	94.256	0.000	21.926	27.147	0.027	0.280	0.011	0.634	2.397	3.957	0.028
6	108.682	0.842	9.012	11.079	0.019	0.189	0.007	0.243	1.019	1.466	0.003
7	60.554	0.000	4.475	5.761	0.015	0.131	0.007	0.103	0.546	0.723	0.009
8	47.686	0.000	2.976	3.914	0.013	0.098	0.010	0.068	0.360	0.470	0.007
9	0.679	0.000	2.100	2.911	0.012	0.076	0.007	0.054	0.269	0.342	0.003
10	52.396	0.417	5.612	8.090	0.017	0.174	0.008	0.123	0.462	0.605	0.008

MOUDI STAGE	CR ug/cm2	MN ug/cm2	FE ug/cm2	CO ug/cm2	NI ug/cm2	CU ug/cm2	ZN ug/cm2	SE ug/cm2	BR ug/cm2	SR ug/cm2	PBL ug/cm2
1	0.010	0.092	3.442	0.007	0.007	0.051	0.012	0.001	0.012	0.001	0.020
2	0.121	1.293	51.646	0.265	0.011	0.934	0.048	0.006	0.004	0.109	0.072
3	0.039	0.465	18.989	0.122	0.010	0.245	0.030	0.011	0.015	0.042	0.028
4	0.050	0.345	12.762	0.082	0.023	0.193	0.032	0.011	0.014	0.088	0.021
5	0.030	0.262	10.420	0.045	0.016	0.147	0.017	0.008	0.014	0.026	0.024
6	0.012	0.091	3.078	0.016	0.008	0.048	0.008	0.009	0.013	0.010	0.009
7	0.008	0.043	1.270	0.003	0.004	0.026	0.004	0.009	0.012	0.032	0.020
8	0.005	0.019	0.675	0.005	0.004	0.017	0.002	0.009	0.012	0.004	0.020
9	0.006	0.011	0.528	0.008	0.004	0.006	0.003	0.008	0.010	0.029	0.004
10	0.003	0.022	1.189	0.012	0.005	0.020	0.009	0.009	0.013	0.005	0.020

# IBA results, coal BL Air Fired

MOUDI	F(197)	Na(440)	AL	SI	P	S	CL	K	CA	TI	V
STAGE	ug/cm2	ug/cm2	ug/cm2	ug/cm2	ug/cm2	ug/cm2	ug/cm2	ug/cm2	ug/cm2	ug/cm2	ug/cm2
1	0.563	0.498	17.605	26.502	0.026	0.625	0.016	0.447	1.664	2.200	0.014
2	234.575	0.000	37.355	57.405	0.002	1.569	0.070	1.062	3.757	5.355	0.022
3	287.910	0.890	47.795	67.904	0.050	0.877	0.029	2.190	5.845	8.110	0.083
4	93.732	1.105	31.551	41.530	0.009	0.336	0.018	1.517	3.584	5.365	0.025
5	71.021	0.481	18.818	23.523	0.007	0.192	0.009	0.879	2.140	3.288	0.040
6	7.097	0.230	8.938	10.630	0.018	0.105	0.008	0.334	0.948	1.311	0.012
7	80.201	0.000	3.772	4.497	0.001	0.057	0.008	0.110	0.343	0.452	0.008
8	0.647	0.392	3.223	3.940	0.013	0.034	0.007	0.088	0.298	0.379	0.007
9	0.609	0.578	2.635	3.224	0.004	0.039	0.002	0.070	0.248	0.313	0.001
10	0.612	0.000	5.788	7.313	0.004	0.111	0.007	0.144	0.427	0.529	0.008

MOUDI	CR	MN	FE	CO	NI	CU	ZN	SE	BR	SR	PBL
STAGE	ug/cm2	ug/cm2	ug/cm2	ug/cm2	ug/cm2	ug/cm2	ug/cm2	ug/cm2	ug/cm2	ug/cm2	ug/cm2
1	0.025	0.179	7.669	0.020	0.007	0.115	0.015	0.008	0.011	0.013	0.005
2	0.057	0.551	23.534	0.128	0.021	0.617	0.040	0.012	0.005	0.075	0.044
3	0.083	0.723	29.999	0.158	0.024	0.748	0.049	0.018	0.018	0.080	0.009
4	0.036	0.418	17.759	0.102	0.012	0.337	0.037	0.011	0.001	0.133	0.022
5	0.023	0.235	9.688	0.052	0.010	0.160	0.029	0.009	0.013	0.035	0.010
6	0.008	0.084	3.123	0.004	0.007	0.050	0.003	0.008	0.011	0.038	0.006
7	0.003	0.029	0.968	0.003	0.004	0.025	0.004	0.010	0.013	0.007	0.020
8	0.004	0.016	0.757	0.010	0.004	0.008	0.001	0.008	0.010	0.015	0.017
9	0.004	0.014	0.694	0.002	0.002	0.011	0.002	0.003	0.010	0.028	0.017
10	0.003	0.026	1.206	0.003	0.004	0.017	0.004	0.002	0.001	0.018	0.004

# IBA results, coal MN Air Fired

MOUDI	F(197)	Na(440)	AL	SI	P	S	CL	K	CA	TI	V
STAGE	ug/cm2	ug/cm2	ug/cm2	ug/cm2	ug/cm2	ug/cm2	ug/cm2	ug/cm2	ug/cm2	ug/cm2	ug/cm2
1	19.915	0.712	11.649	26.437	0.091	0.553	0.010	1.808	0.504	0.943	0.008
2	0.589	0.000	22.154	51.539	0.135	1.244	0.011	3.341	1.331	2.152	0.021
3	0.565	0.797	19.385	43.370	0.106	0.788	0.010	2.747	0.971	1.577	0.014
4	0.611	0.627	21.608	43.880	0.106	0.650	0.010	2.830	1.085	1.803	0.014
5	0.648	0.000	12.927	24.641	0.062	0.419	0.009	1.614	0.608	1.014	0.011
6	0.576	0.530	7.478	14.068	0.021	0.833	0.036	1.155	0.483	0.869	0.011
7	0.564	0.295	4.048	7.619	0.004	0.675	0.022	0.604	0.237	0.387	0.006
8	37.251	0.000	4.035	7.851	0.013	0.686	0.007	0.583	0.221	0.403	0.008
9	0.651	0.578	1.626	3.056	0.006	0.213	0.008	0.185	0.093	0.173	0.006
10	30.783	0.000	2.653	4.395	0.007	0.210	0.008	0.241	0.134	0.212	0.006

MOUDI	CR	MN	FE	CO	NI	CU	ZN	SE	BR	SR	PBL
STAGE	ug/cm2	ug/cm2	ug/cm2	ug/cm2	ug/cm2	ug/cm2	ug/cm2	ug/cm2	ug/cm2	ug/cm2	ug/cm2
1	0.007	0.058	3.980	0.020	0.001	0.042	0.005	0.009	0.004	0.063	0.020
2	0.017	0.197	11.281	0.066	0.014	0.169	0.016	0.009	0.013	0.196	0.002
3	0.007	0.110	6.562	0.024	0.011	0.121	0.014	0.001	0.010	0.186	0.015
4	0.020	0.134	6.639	0.032	0.002	0.135	0.028	0.008	0.011	0.176	0.017
5	0.007	0.065	3.456	0.022	0.003	0.051	0.016	0.008	0.001	0.060	0.018
6	0.013	0.056	2.946	0.022	0.015	0.042	0.028	0.001	0.010	0.074	0.002
7	0.004	0.024	1.425	0.002	0.008	0.013	0.011	0.001	0.009	0.020	0.011
8	0.002	0.022	1.340	0.013	0.005	0.011	0.017	0.008	0.010	0.022	0.020
9	0.006	0.003	0.480	0.008	0.003	0.008	0.008	0.008	0.011	0.002	0.018
10	0.004	0.007	0.570	0.009	0.004	0.021	0.003	0.009	0.012	0.003	0.020



# IBA results, coal CL Oxy Fired

MOUDI	F(197)	Na(440)	AL	SI	P	S	CL	K	CA	TI	V
STAGE	ug/cm2	ug/cm2	ug/cm2	ug/cm2	ug/cm2	ug/cm2	ug/cm2	ug/cm2	ug/cm2	ug/cm2	ug/cm2
1	0.582	0.287	2.095	3.340	0.012	0.042	0.007	0.120	0.121	0.224	0.006
2	0.627	0.425	18.376	30.682	0.030	0.245	0.008	1.196	1.532	2.326	0.013
3	0.617	0.773	40.768	59.646	0.039	0.122	0.009	2.275	2.946	5.413	0.029
4	0.617	0.680	7.487	12.741	0.023	0.082	0.007	0.589	0.264	0.531	0.008
5	57.095	0.283	20.457	24.975	0.026	0.100	0.009	1.393	1.271	2.979	0.015
6	246.792	0.000	7.103	8.158	0.017	0.055	0.009	0.364	0.400	0.903	0.002
7	184.740	0.000	1.568	1.974	0.001	0.016	0.008	0.069	0.069	0.144	0.006
8	172.086	0.000	0.583	0.735	0.010	0.011	0.008	0.024	0.025	0.043	0.006
9	183.375	0.000	0.242	0.331	0.010	0.008	0.008	0.010	0.003	0.024	0.001
10	16.017	0.510	0.151	0.184	0.009	0.007	0.007	0.009	0.008	0.018	0.005

MOUDI	CR	MN	FE	CO	NI	CU	ZN	SE	BR	SR	PBL
STAGE	ug/cm2	ug/cm2	ug/cm2	ug/cm2	ug/cm2	ug/cm2	ug/cm2	ug/cm2	ug/cm2	ug/cm2	ug/cm2
1	0.004	0.009	0.603	0.004	0.001	0.001	0.003	0.008	0.010	0.028	0.016
2	0.012	0.231	9.546	0.043	0.012	0.061	0.014	0.009	0.012	0.064	0.000
3	0.035	0.452	19.259	0.092	0.018	0.162	0.032	0.011	0.013	0.266	0.036
4	0.007	0.033	1.789	0.003	0.005	0.018	0.010	0.002	0.010	0.026	0.014
5	0.011	0.187	8.958	0.031	0.009	0.080	0.034	0.009	0.012	0.103	0.018
6	0.033	0.055	2.396	0.003	0.013	0.023	0.018	0.010	0.014	0.005	0.022
7	0.001	0.002	0.342	0.007	0.004	0.004	0.001	0.010	0.013	0.035	0.021
8	0.003	0.001	0.111	0.005	0.004	0.003	0.002	0.011	0.014	0.039	0.023
9	0.002	0.001	0.047	0.004	0.003	0.003	0.003	0.010	0.013	0.035	0.022
10	0.004	0.003	0.033	0.003	0.003	0.003	0.003	0.009	0.012	0.031	0.007

# IBA results, coal BL Oxy Fired

MOUDI	F(197)	Na(440)	AL	SI	P	S	CL	K	CA	TI	V
STAGE	ug/cm2	ug/cm2	ug/cm2	ug/cm2	ug/cm2	ug/cm2	ug/cm2	ug/cm2	ug/cm2	ug/cm2	ug/cm2
1	72.332	0.000	10.338	15.543	0.033	0.422	0.009	0.629	1.033	1.176	0.011
2	137.749	0.000	20.540	31.325	0.063	0.400	0.010	1.150	2.172	2.592	0.016
3	63.596	0.971	26.386	38.743	0.085	0.313	0.003	1.610	2.262	2.952	0.002
4	69.169	0.433	21.666	29.913	0.041	0.261	0.011	1.394	1.359	2.247	0.014
5	0.657	1.186	17.837	22.356	0.035	0.237	0.024	1.611	1.438	3.004	0.001
6	145.283	0.000	7.936	9.341	0.016	0.120	0.008	0.653	0.551	1.365	0.012
7	20.664	0.307	2.972	3.656	0.001	0.059	0.008	0.187	0.153	0.391	0.007
8	0.610	0.000	1.825	2.364	0.011	0.076	0.002	0.098	0.090	0.197	0.006
9	0.552	1.004	1.086	1.457	0.010	0.117	0.007	0.055	0.050	0.108	0.003
10	58.133	0.000	1.172	1.503	0.011	0.056	0.004	0.042	0.045	0.084	0.005

MOUDI	CR	MN	FE	CO	NI	CU	ZN	SE	BR	SR	PBL
STAGE	ug/cm2	ug/cm2	ug/cm2	ug/cm2	ug/cm2	ug/cm2	ug/cm2	ug/cm2	ug/cm2	ug/cm2	ug/cm2
1	0.006	0.119	5.613	0.014	0.010	0.025	0.005	0.009	0.006	0.055	0.005
2	0.017	0.292	12.559	0.046	0.017	0.102	0.016	0.010	0.014	0.026	0.023
3	0.007	0.272	12.893	0.062	0.013	0.059	0.018	0.010	0.013	0.096	0.021
4	0.008	0.186	8.091	0.043	0.007	0.070	0.026	0.004	0.013	0.065	0.011
5	0.012	0.227	10.925	0.066	0.011	0.074	0.048	0.010	0.013	0.091	0.003
6	0.004	0.094	4.158	0.031	0.008	0.024	0.017	0.009	0.012	0.032	0.019
7	0.004	0.014	0.953	0.011	0.005	0.007	0.001	0.001	0.011	0.031	0.019
8	0.002	0.006	0.440	0.008	0.003	0.004	0.003	0.007	0.009	0.026	0.016
9	0.004	0.007	0.262	0.006	0.003	0.003	0.001	0.008	0.005	0.027	0.017
10	0.003	0.002	0.212	0.006	0.003	0.003	0.003	0.009	0.012	0.019	0.020

# IBA results, coal MN Oxy Fired

MOUDI	F(197)	Na(440)	AL	SI	P	S	CL	K	CA	TI	V
STAGE	ug/cm2	ug/cm2	ug/cm2	ug/cm2	ug/cm2	ug/cm2	ug/cm2	ug/cm2	ug/cm2	ug/cm2	ug/cm2
1	0.602	0.000	11.648	25.570	0.113	1.430	0.003	2.009	0.661	1.079	0.001
2	0.586	0.732	39.097	80.959	0.287	2.678	0.022	6.487	3.621	5.117	0.069
3	0.600	1.615	45.850	97.039	0.329	2.853	0.001	9.073	3.444	6.076	0.122
4	36.016	0.704	34.353	65.899	0.195	1.745	0.021	6.356	2.059	4.161	0.049
5	157.393	0.000	18.324	33.921	0.100	1.013	0.021	3.774	1.098	2.597	0.059
6	89.457	0.368	9.421	15.587	0.052	0.506	0.011	1.488	0.575	1.225	0.012
7	141.261	0.000	3.764	6.225	0.023	0.376	0.009	0.499	0.205	0.437	0.008
8	112.921	0.396	4.325	8.010	0.021	1.080	0.018	0.761	0.235	0.486	0.009
9	54.613	0.000	1.585	2.762	0.012	0.758	0.009	0.226	0.120	0.210	0.007
10	0.636	0.323	3.479	4.926	0.013	0.575	0.041	0.242	0.238	0.325	0.001

MOUDI	CR	MN	FE	CO	NI	CU	ZN	SE	BR	SR	PBL
STAGE	ug/cm2	ug/cm2	ug/cm2	ug/cm2	ug/cm2	ug/cm2	ug/cm2	ug/cm2	ug/cm2	ug/cm2	ug/cm2
1	0.008	0.086	5.600	0.030	0.009	0.081	0.007	0.008	0.011	0.099	0.018
2	0.023	0.600	31.654	0.152	0.020	0.655	0.054	0.002	0.012	0.396	0.023
3	0.007	0.502	28.395	0.162	0.013	0.616	0.064	0.004	0.015	0.645	0.081
4	0.028	0.320	18.402	0.112	0.002	0.344	0.026	0.005	0.016	0.548	0.019
5	0.026	0.229	12.073	0.060	0.009	0.211	0.026	0.005	0.008	0.325	0.022
6	0.005	0.091	4.271	0.021	0.009	0.111	0.007	0.009	0.006	0.126	0.020
7	0.004	0.031	1.476	0.009	0.006	0.045	0.005	0.009	0.012	0.023	0.021
8	0.007	0.026	1.862	0.006	0.009	0.049	0.001	0.005	0.011	0.065	0.007
9	0.004	0.012	0.722	0.010	0.011	0.031	0.003	0.009	0.012	0.031	0.020
10	0.003	0.018	0.945	0.011	0.002	0.062	0.005	0.008	0.003	0.013	0.016

